Supporting Information

Histone H4 tails in nucleosomes: a fuzzy interaction with DNA

Sevastyan O. Rabdano,[1] Matthew D. Shannon,[2] Sergei A. Izmailov,[1] Nicole Gonzalez Salguero,[2] Mohamad Zandian,[2] Rudra N. Purusottam,[2] Michael G. Poirier,[3] Nikolai R. Skrynnikov,[1,4]✉ and Christopher P. Jaroniec[2]✉

[1] Laboratory of Biomolecular NMR, St. Petersburg State University, St. Petersburg 199034, Russia

[2] Department of Chemistry and Biochemistry, The Ohio State University, Columbus, Ohio 43210, United States

[3] Department of Physics, The Ohio State University, Columbus, Ohio 43210, United States

[4] Department of Chemistry, Purdue University, West Lafayette, Indiana 47906, United States

✉ n.skrynnikov@spbu.ru and jaroniec.1@osu.edu

Materials and Methods

***Nucleosome samples*.** NCP samples were prepared using established protocols.[1] *Xenopus laevis* histones H2A, H2B, H3 and H4 were overexpressed in *E. coli* BL21 (DE3) pLysS cells. Cells were grown in either LB medium for unlabeled samples or M9 minimal medium supplemented with $^{15}NH_4Cl$ or $^{15}NH_4Cl$ + [$^{13}C_6$]glucose for ^{15}N- or $^{15}N/^{13}C$-enriched samples. Histones were obtained in a form of inclusion bodies, refloated with 7 M urea, purified using ion-exchange and gel-filtration chromatography and then lyophilized. To prepare histone octamers, H2A, H2B, H3 and H4 histones were combined with molar ratio 1.2:1.2:1:1 in denaturing buffer (20 mM Tris pH 7.5, 7 M GuHCl, 10 mM DTT buffer), dialyzed into refolding buffer (10 mM Tris pH 7.5, 2 M NaCl, 1 mM EDTA, 5 mM BME) and purified via gel-filtration chromatography. pJ201 plasmid containing 32 repeats of the 147 bp Widom 601 sequence (see Figure S1) was amplified in *E. coli* and purified via alkaline lysis. The Widom 601 fragments were released by cleavage with EcoRV and separated from parent plasmid by polyethylene glycol precipitation. NCPs were reconstituted by mixing 147 bp Widom 601 DNA and histone octamers at a 1:0.65 molar ratio, desalted using a salt gradient, purified using a 5–30% sucrose gradient and buffer exchanged into NMR buffer (see below). Nucleosome concentration was determined using UV absorbance at 260 nm from the Widom 601 DNA.

NMR experiments. NMR measurements were conducted at 25 °C using the samples containing 50 μM of NCP in a buffered solution with pH 7 (95% H_2O / 5% D_2O, 5 mM Tris, 100 mM NaCl, 0.5 mM EDTA, 0.1 mM $MgCl_2$). All experiments were recorded on a Bruker Avance III HD Ascend 850 MHz spectrometer. Spectral assignment was accomplished by means of HNCA, HN(CO)CA and HNCACB[2] experiments. ^{15}N relaxation measurements were conducted using the recently reported improved versions of the standard HSQC-based pulse sequences.[3] Additionally, a CPMG experiment[4] was conducted to rule out the effect of exchange broadening and pulsed-field gradient diffusion measurements[5] were carried out to confirm the integrity of NCPs. Experimental spin relaxation rates and backbone chemical shifts are summarized in Table S1. In addition to seven unambiguously assigned $^1H^N$,^{15}N-HSQC resonances, three lysine signals can be tentatively assigned based on assignments of the free N-H4 peptide (see Figure S3) and their measured relaxation rates. It appears that K12 is highly mobile, $R_2 = 11 \pm 2\ s^{-1}$, while K5 and K8 are more constrained, $R_2 = 16 \pm 5$ and $17 \pm 2\ s^{-1}$. This picture is broadly consistent with the (Amber ff14SB / TIP4P-D) model. Finally, there is also a heavily overlapped glycine peak, G4/G6/G13, where one may expect that its effective relaxation rate is dominated by the more mobile and slowly relaxing residue (G13). These expectations are borne out, with a measured R_2^{eff} of $12\ s^{-1}$.

MD simulations. MD trajectories have been recorded using Amber 18 package with Amber ff14SB force field. The initial NCP coordinates were constructed based on the crystallographic structure 3LZ0. To rebuild the histone tails, which are missing from this structure (indicated by over- and underbars in Figure S1), we have generated 5,000 random-coil-like chains using for this purpose programs OOPS[6] and SCWRL4.[7] The chains contained all tail residues that are absent from the crystal structure, plus the first N-terminal residue whose coordinates are found in the structure (for N-terminal tails) or the last C-terminal residue whose coordinates are found in the structure in (for C-terminal tails). The so generated tails were "glued" onto the body of the corresponding histone by

superimposing N, C^{α} and C' atoms in the overlapping residues.[8] The resulting NCP structures were protonated in accordance with the experimental pH using program PDB2PQR.[9] The structures were then energy-minimized and their energies were evaluated in implicit GB-Neck2 solvent (igb=8 option in Amber).[10] 40 structures with the lowest energies were selected for further analysis and solvated with TIP4P-D water (5 Å minimal separation between the NCP atoms and the boundary of truncated octahedron box). Na^+ and Cl^- ions have been added to neutralize the system and to match 100 mM NaCl concentration in the experimental sample.[11] Out of 40 realizations of the simulation cell, the one with the biggest size was chosen to start the trajectory (diameter of inscribed sphere d_i = 229 Å). After 30-ns initial run, all tails adopted more compact conformations; at this point, the simulation was stopped and the system was resolvated (d_i = 170 Å, number of water molecules in the cell 104,832). The size of the simulation cell and the separation between the "master copy" of NCP and its periodic images is illustrated in Figure S18. This configuration was used to start the production run. The first 50 ns of the trajectory were treated as an equilibration period and excluded from the data analyses. The trajectory was inspected for contacts of NCP with its periodic images (via fully extended histone tails). None has been found in this particular simulation, but we observed formation of such contacts in other trajectories. During the simulations, the equations of motion were integrated using the leapfrog algorithm with a time step of 2 fs. Bonds involving hydrogen atoms were constrained using SHAKE algorithm.[12] The non-bonded interactions were calculated with cutoff of 10.5 Å, as recommended for disordered proteins.[13] Long-range interactions were treated using a particle-mesh Ewald summation scheme[14] with default parameters for grid spacing and spline interpolation. Constant pressure was maintained using Berendsen barostat[15] with relaxation time 2 ps. Langevin thermostat with collision frequency 2 ps^{-1} was used to stabilize temperature at 25°C. The same protocol was used for (Amber ff14SB / TIP3P) simulation, including the size of the simulation cell that was identical to (Amber ff14SB / TIP4P-D) trajectory. The analogous setup was also used for other simulations: (Amber ff15ipq / SPC/Eb), (CHARMM c36m / CHARMM-modified TIP3P), (CHARMM c36m + CUFIX / CHARMM-modified TIP3P), (Amber ff14SB + the latest version of CUFIX / TIP3P), etc. One trajectory was recorded using Gromacs platform[16] using the exact same protocol as described by You *et al*.[17]

Calculation of chemical shifts. $^{1}H^{N}$, ^{15}N and $^{13}C^{\alpha/\beta}$ chemical shifts were calculated for individual MD frames using the program SHIFTX2. Additionally, SHIFTS calculations were performed to capture potential shifts due to interactions of N-H4 tails with nDNA. Specifically, SHIFTS calculation were conducted for (*i*) complete NCP structure extracted from an MD frame and (*ii*) histone component only. The difference between (*i*) and (*ii*) was taken to be an nDNA contribution and added to the SHIFTX2 result. The calculated shifts were averaged over a series of frames spaced at the interval 1 ns.

Calculation of relaxation rates. The MD frames were initially superimposed onto the reference structure 3LZ0 by overlaying the secondary-structure C^{α} atoms from the histone core. The dipolar (CSA) time-correlation functions $C_{NH}(t) = \langle P_2(\cos\chi(t)) \rangle$ [18] for amide N-H^N vectors in N-terminal H4 tails have been calculated using fast Fourier transformation.[19] To reintroduce the effect of the overall NCP tumbling, the results were multiplied by $exp(-\tau/\tau_{rot})$, where τ_{rot} is the tumbling correlation time obtained by application of HYDROPRO to the trajectory at hand (for

the purpose of HYDROPRO calculations, the trajectory was sampled at 1 ns intervals). The obtained $C_{NH}(t)$ curves were fitted with a 6-exponential function, containing twelve fitting parameters (amplitudes a_i and characteristic times τ_i). For the purpose of fitting, the correlation function was resampled on a non-uniform grid extending from 0 to 759 ns. The grid was constructed using a scaling factor 1.005: t_0=0, t_1=1 ps, t_{k+1}=ceil(t_k*1.005). The fitting was performed using Levenberg-Marquardt algorithm implemented in SciPy function *curve_fit*.[20] As an initial approximation, we have used a_i = 1/6 and τ_i uniformly distributed on a logarithmic scale between 1 ps and 163.4 ns; prior to the fitting, these values were subjected to a random variation. For each correlation function, the fitting was repeated thrice with the randomized initial conditions. The outcome of the fitting procedure proved stable and reproducible. The obtained a_i and τ_i values were translated into spectral densities, which were in turn used to calculate ^{15}N R_1 and R_2 relaxation rates.[21] In these calculations, we employed the standard values of the N-H^N bond length (1.02 Å) and ^{15}N chemical shift anisotropy (-170 ppm).[22]

Calculation of gyration radius. The NCP coordinates were extracted from the trajectory with the step of 1 ns. These coordinates were further processed using the program CRYSOL to generate per-frame scattering intensity profiles $I(q)$. The calculations were performed using the default value for hydration-shell electron density contrast, 0.03 e/Å^3, which appears to be a reasonable setting for nucleosome.[23] The per-frame $I(q)$ profiles were summed and then analyzed using the program GNOM to extract R_g.

Identification of hydrogen bonds and salt bridges. NCP coordinates have been extracted with 100 ps step and processed to identify hydrogen bonds and salt bridges originating on N-H4 tails. Hydrogen bonds were detected using HBPLUS.[24] Since HBPLUS was originally designed to deal with mononucleotides, the obtained list of hydrogen bonds required some additional filtering. Salt bridges were identified using in-house script; the criterion was that at least one nitrogen-to-oxygen distance in the ion pair must be less than 4 Å (for DNA phosphate groups, only OP1 and OP2 atoms were taken into consideration, but not O3' and O5', see Figure S6 for details). To generate Figure 3, we have divided the entire trajectory into 5-ns intervals. For each interval, we have determined the content of a given interaction (hydrogen bond or a salt bridge). If the interaction is present at the level greater than 20% in at least one interval, it is included in the plot and represented with a band (the width of all bands is the same). The bands are colored using one of the four shades, from pale to dark, according to the content of the given interaction in the 5-ns interval: 0.2-0.4, 0.4-0.6, 0.6-0.8, 0.8-1.0. If two interacting moieties had formed simultaneously a salt bridge and a hydrogen bond (which is a common occurrence), then only the former is shown in the plot.

Calculation of rmsf and minimal separation between N-H4 tails and the body of nucleosome. The MD frames were initially superimposed onto the reference structure 3LZ0 by overlaying the secondary-structure C^α atoms from the histone core. Rmsf values were calculated for C^α atoms from residues 1-24 in N-H4 tails. The minimal distance between the selected residue in the N-H4 tail and the remaining portion of the nucleosome was found using k-d tree algorithm[25] in SciPy. This minimal distance was then averaged over a series of MD frames (spaced at 100 ps).

Tables

Table S1. Relaxation rates of amide ^{15}N and chemical shifts of $^{1}H^{N}$, ^{15}N and $^{13}C^{\alpha/\beta}$ atoms in histone H4.

Residue	R_1, s^{-1}	R_2, s^{-1}	δH^N, ppm	δN, ppm	δC^α, ppm	δC^β, ppm
R3	1.27	16.4	8.500	120.775	56.425	30.926
G7	1.29	12.4	8.338	108.846	45.365	
G9	1.17	11.6	8.545	109.823	45.386	
L10	1.21	12.5	8.206	121.442	55.251	42.415
G11	1.18	11.0	8.517	109.533	45.362	
G14	1.23	9.9	8.302	108.902	45.151	
A15	1.20	20.3	8.230	123.793	52.455	19.464

Table S2. Annotation of the interactions shown in Figure 3. Hydrogen bonds are listed using full labels for the donor and acceptor atoms. Salt bridges are listed using a shortened format that does not specify atom types (for N-H4, ionic groups are uniquely identified by residue type and number; for nDNA, only phosphate groups are involved in salt bridges). Standard nucleotides are labeled dA, dT, dC and dG. Nucleotide numbering is from -72 to 72, same as in the structure PDB ID 3LZ0. Peptide chains and nucleotide strands are labeled A-J, same as in 3LZ0. For each interaction, we also list its net content across the entire trajectory (expressed in percentage points). Those interactions with net content greater than 5% are highlighted.

N-H4-1

S1 - D81 (A), [0.2%]
S1 - DA-22 (I), [0.1%]
S1 - DC-29 (I), [0.9%]
S1 - DG-30 (I), [0.3%]
S1 OG - DC-29 OP1 (I), [0.2%]
S1 - DA-31 (I), [0.5%]
S1 OG - DT35 OP1 (J), [0.1%]
S1 N - DC-32 O3' (I), [0.1%]
S1 - DT35 (J), [0.1%]
S1 - DC34 (J), [0.3%]
S1 N - DG27 N7 (J), [2.1%]
S1 OG - DA26 OP2 (J), [1.7%]
S1 N - DA26 N7 (J), [0.8%]
S1 N - DG27 O6 (J), [0.9%]
S1 - DT-28 (I), [15.2%]
S1 - DT33 (J), [2.2%]
S1 OG - DC24 OP2 (J), [0.3%]
S1 - DG23 (J), [0.2%]
S1 OG - K21 NZ (H), [0.2%]
S1 - DC-27 (I), [0.9%]
S1 N - Q19 OE1 (H), [0.1%]
S1 OG - DC-27 OP2 (I), [0.1%]
S1 O - D22 N (H), [0.1%]
S1 OG - DT-28 OP1 (I), [2.8%]
S1 OG - K2 NZ (H), [0.2%]
S1 OG - DT33 OP1 (J), [0.8%]
S1 OG - DG32 O3' (J), [0.5%]
S1 OG - DG32 OP1 (J), [0.7%]
S1 - DG32 (J), [1.2%]
S1 OG - DC-29 O3' (I), [0.7%]
S1 N - DT31 O3' (J), [0.3%]
S1 OG - DT31 O3' (J), [0.1%]
G2 N - DA-31 OP1 (I), [0.2%]
G2 N - DG27 O6 (J), [0.3%]
G2 N - DA26 OP2 (J), [0.1%]
G2 N - DC-27 OP2 (I), [0.3%]
G2 O - K21 NZ (H), [0.2%]
G2 N - DC-29 OP1 (I), [0.2%]
G2 O - K2 NZ (H), [0.2%]
G2 N - DT33 OP1 (J), [0.8%]
G2 N - DT-28 OP1 (I), [0.7%]
G2 N - DG32 OP1 (J), [0.7%]
G2 N - DG32 O5' (J), [0.1%]
R3 - D81 (A), [2.7%]
R3 - DA26 (J), [0.2%]
R3 - DT25 (J), [0.6%]
R3 - DC-29 (I), [2.2%]
R3 - DG-30 (I), [2.5%]
R3 - DT-28 (I), [0.5%]
R3 - D22 (H), [0.4%]
R3 NH1 - DT25 O4 (J), [0.1%]
R3 - DC24 (J), [0.2%]
R3 - DC-27 (I), [0.1%]
R3 - DG23 (J), [0.1%]
R3 NH1 - DG27 O6 (J), [0.1%]
R3 NH1 - DA-25 N7 (I), [0.1%]
R3 - DT-26 (I), [2.5%]
R3 - DA-25 (I), [0.1%]
R3 NH1 - K21 O (H), [0.2%]
R3 NE - K21 O (H), [0.3%]
R3 NE - K20 O (H), [0.2%]
R3 NH1 - K20 O (H), [0.5%]
R3 NH2 - DA-31 O3' (I), [0.1%]
R3 NH1 - DA-31 O4' (I), [9.0%]
R3 - DC34 (J), [0.7%]
R3 NH1 - DA-31 N3 (I), [6.1%]
R3 NH2 - DA-31 N3 (I), [14.5%]
R3 NH2 - DA-31 O4' (I), [0.2%]
R3 NH1 - DG-30 N3 (I), [0.2%]
R3 NH1 - DG32 O4' (J), [1.2%]
R3 NE - DT31 O2 (J), [1.7%]
R3 NH1 - DG32 N3 (J), [1.4%]
R3 NH1 - DT31 O2 (J), [40.2%]
R3 N - DG32 OP1 (J), [1.5%]
R3 NH1 - DT33 O4' (J), [0.2%]
R3 NE - DG32 O4' (J), [0.4%]
R3 N - DT31 O3' (J), [0.2%]
R3 NH2 - DG-30 O4' (I), [0.2%]
R3 NH2 - DG-30 N3 (I), [0.5%]
R3 N - DG32 O3' (J), [12.0%]
R3 N - DT33 OP1 (J), [11.1%]
R3 NH2 - DG32 N3 (J), [1.5%]
R3 NH2 - DT31 O2 (J), [42.9%]
R3 NH1 - DT31 O4' (J), [7.3%]
R3 NH2 - DG32 O4' (J), [0.6%]
G4 N - DT25 OP2 (J), [0.3%]
G4 N - DG-30 O3' (I), [33.0%]
G4 N - DC-29 OP1 (I), [20.8%]
G4 N - DT33 OP1 (J), [9.0%]
K5 - D81 (A), [0.1%]
K5 - DA26 (J), [0.4%]
K5 - DC-29 (I), [0.3%]
K5 NZ - DG27 O6 (J), [0.1%]
K5 NZ - DG27 N7 (J), [0.2%]
K5 NZ - DA26 N7 (J), [0.1%]
K5 - DG-30 (I), [1.4%]
K5 - DA-31 (I), [0.4%]
K5 - D22 (H), [0.1%]
K5 - DC-27 (I), [0.6%]
K5 - DC24 (J), [0.5%]
K5 - DT-28 (I), [0.1%]
K5 O - DC-27 N4 (I), [0.4%]
K5 NZ - A1 O (H), [0.1%]
K5 - DC34 (J), [10.2%]
K5 - DT33 (J), [0.6%]
G6 N - DG-30 OP1 (I), [3.1%]
G6 N - DG-30 OP2 (I), [1.5%]
G6 N - DG-30 O5' (I), [0.6%]
G6 N - DC-29 OP2 (I), [0.8%]
G6 N - DC34 OP1 (J), [3.8%]
G6 N - DT33 O3' (J), [3.3%]
G7 N - DC-29 OP2 (I), [0.6%]
G7 N - DT-26 O4 (I), [0.2%]
G7 O - DC-27 N4 (I), [0.7%]
G7 N - DG-30 OP2 (I), [1.7%]
G7 N - DG-30 OP1 (I), [2.8%]
G7 N - DA-31 O3' (I), [0.5%]
K8 - DT25 (J), [0.6%]
K8 - DC-20 (I), [0.1%]
K8 - DA26 (J), [0.8%]
K8 - D81 (A), [0.4%]
K8 - DC24 (J), [0.4%]
K8 NZ - DG27 N7 (J), [3.8%]
K8 NZ - DG27 O6 (J), [2.6%]
K8 NZ - DA26 N7 (J), [0.3%]
K8 NZ - DT-28 O4 (I), [1.6%]
K8 - DC-29 (I), [2.3%]
K8 - DG-30 (I), [3.6%]
K8 - DG23 (J), [0.4%]
K8 - DA-31 (I), [4.3%]
K8 N - DG27 O6 (J), [0.1%]
K8 O - DC-27 N4 (I), [0.2%]
G9 N - DC24 OP1 (J), [0.1%]
G9 N - DC-29 OP2 (I), [0.4%]
G9 N - DG-30 OP2 (I), [0.7%]
G9 N - DG-30 OP1 (I), [2.2%]
G9 N - DA-31 O3' (I), [4.0%]
L10 N - DG27 O6 (J), [2.4%]
L10 N - DG-30 OP2 (I), [0.4%]
L10 N - DG-30 OP1 (I), [0.3%]
G11 N - DG-30 OP2 (I), [0.2%]
K12 - DA26 (J), [2.9%]
K12 - DT25 (J), [9.0%]
K12 NZ - DC-23 O3' (I), [0.2%]
K12 - D81 (A), [0.4%]
K12 - DA-22 (I), [0.6%]
K12 - DG27 (J), [0.5%]
K12 - DC24 (J), [0.7%]
K12 - DC-20 (I), [0.3%]
K12 NZ - DC-21 O3' (I), [0.2%]
K12 - DG23 (J), [0.2%]
K12 - DA-31 (I), [0.3%]
K12 - DG-30 (I), [0.5%]
K12 NZ - DG27 N7 (J), [1.0%]
K12 NZ - DA26 N7 (J), [0.7%]
K12 NZ - DG27 O6 (J), [0.9%]
K12 NZ - DT-28 O4 (I), [0.3%]
G13 N - DA26 OP1 (J), [0.3%]
G13 N - DA26 OP2 (J), [1.3%]
G13 N - DT25 OP2 (J), [0.2%]
G14 N - DT25 OP1 (J), [0.3%]
G14 N - DA26 OP1 (J), [0.9%]
G14 N - DT25 OP2 (J), [0.1%]
G14 N - DA26 O5' (J), [0.5%]
A15 N - DT25 OP1 (J), [1.5%]
K16 - DT25 (J), [7.8%]
K16 - DA26 (J), [17.9%]
K16 - DG27 (J), [2.3%]
K16 - DC-20 (I), [0.5%]
K16 - DC24 (J), [0.1%]
K16 - DC-21 (I), [0.9%]
K16 - DG-19 (I), [0.3%]
K16 - DA-22 (I), [3.9%]
K16 NZ - DA-22 N3 (I), [0.2%]
K16 NZ - DA-22 O4' (I), [0.1%]
K16 NZ - T80 O (A), [0.1%]
K16 - D81 (A), [9.6%]
K16 NZ - DC-23 O3' (I), [0.3%]
R17 NH2 - DA-22 N3 (I), [0.9%]
R17 - DC-20 (I), [4.1%]
R17 NH1 - DA-22 N3 (I), [0.8%]
R17 NE - DC-21 O4' (I), [0.1%]
R17 NH2 - DC24 O3' (J), [1.6%]
R17 - DC-21 (I), [24.3%]
R17 - DT25 (J), [21.9%]
R17 NH1 - DC24 O3' (J), [11.5%]
R17 NE - DC24 O3' (J), [0.8%]
R17 - DA26 (J), [0.6%]
R17 - DG-19 (I), [0.5%]
R17 NH1 - DA-22 O4' (I), [0.5%]
R17 - DA-22 (I), [2.0%]
R17 NH2 - DC-23 O3' (I), [0.1%]
R17 - D81 (A), [0.9%]
R17 NH1 - DC-23 O2 (I), [0.4%]
R17 NH1 - DC24 O2 (J), [0.1%]
R17 NH2 - DC24 O2 (J), [0.1%]
R17 NH2 - DC-23 O2 (I), [0.5%]
H18 ND1 - DC-21 OP1 (I), [1.8%]
H18 ND1 - DA-22 O3' (I), [3.0%]
H18 ND1 - DA-22 OP1 (I), [0.8%]
H18 ND1 - D81 OD2 (A), [0.9%]
H18 ND1 - D81 OD1 (A), [1.5%]
H18 ND1 - DC-21 OP2 (I), [0.3%]
H18 ND1 - DA-22 OP2 (I), [0.1%]
R19 - D81 (A), [16.5%]
R19 - DA-22 (I), [49.9%]
R19 NH2 - D81 O (A), [0.6%]
R19 NH2 - L82 O (A), [0.3%]
R19 - DC-23 (I), [0.6%]
R19 - DC-21 (I), [18.4%]
R19 - DC-20 (I), [2.3%]
R19 - DA17 (J), [0.3%]
R19 - E73 (A), [2.4%]
R19 NH1 - Q76 OE1 (A), [0.9%]
R19 - DT25 (J), [0.3%]
R19 NH1 - R72 O (A), [0.2%]
R19 NH2 - Q76 OE1 (A), [0.5%]
R19 - DA26 (J), [3.7%]
R19 NH1 - L82 O (A), [0.3%]
K20 - DC-21 (I), [8.3%]
K20 - DA-22 (I), [0.3%]
K20 - DA16 (J), [1.1%]
K20 - DC-20 (I), [1.0%]
L22 O - N25 ND2 (B), [44.6%]
L22 O - R69 NH1 (A), [0.1%]
L22 O - Q76 NE2 (A), [1.2%]
L22 N - Q76 OE1 (A), [0.6%]
R23 - E73 (A), [5.9%]
R23 - D77 (A), [2.8%]
R23 - DA16 (J), [1.1%]
R23 NH1 - Q76 OE1 (A), [0.5%]
R23 NH2 - Q76 OE1 (A), [0.9%]
R23 O - R69 NH1 (A), [0.5%]
R23 NE - Q27 OE1 (B), [0.3%]
R23 NH2 - Q27 OE1 (B), [0.2%]
R23 - DC-12 (I), [2.6%]
D24 N - E73 OE2 (A), [23.4%]
D24 O - Q27 N (B), [71.3%]
D24 O - G28 N (B), [25.7%]
D24 N - E73 OE1 (A), [15.9%]
D24 O - Q27 NE2 (B), [0.6%]
D24 O - R69 NH1 (A), [0.2%]

N-H4-2

S1 N - DG-19 N7 (J), [16.1%]
S1 N - DG-19 O6 (J), [8.2%]
S1 OG - DG-18 O6 (J), [3.1%]
S1 OG - DT-17 O4 (J), [1.6%]
S1 OG - DA17 N6 (I), [3.1%]
S1 OG - DA17 N7 (I), [0.3%]
S1 OG - DA16 N7 (I), [0.6%]
S1 OG - DC18 N4 (I), [0.8%]
S1 N - DG-18 O6 (J), [18.5%]
S1 N - DG-18 N7 (J), [10.6%]
S1 N - DT-17 O4 (J), [0.5%]
S1 OG - DG-18 N7 (J), [2.9%]
S1 - DT-17 (J), [0.2%]
S1 OG - DT-17 OP2 (J), [0.4%]
S1 - DT15 (I), [0.2%]
S1 - DT-16 (J), [0.2%]
S1 - DG62 (J), [0.3%]
S1 - DC61 (J), [0.2%]
S1 OG - DG62 OP2 (J), [0.2%]
S1 OG - DC61 OP2 (J), [0.1%]
S1 OG - DG63 OP2 (J), [0.1%]
S1 OG - DA-67 OP2 (I), [0.1%]
S1 - DA-66 (I), [0.2%]
S1 - DG-68 (I), [0.3%]
S1 OG - DG-68 OP2 (I), [0.2%]
S1 OG - DG-68 OP1 (I), [0.2%]
S1 - DA-67 (I), [0.9%]
S1 - DT12 (I), [0.9%]
S1 OG - DT12 OP2 (I), [0.6%]
S1 OG - DT12 OP1 (I), [0.3%]
S1 - DT13 (I), [0.1%]
S1 OG - DG11 OP2 (I), [0.8%]
S1 - DG11 (I), [0.7%]
S1 OG - DG-19 O6 (J), [1.1%]
S1 OG - DG-19 N7 (J), [0.8%]
S1 OG - DC-20 N4 (J), [0.2%]
S1 OG - DC-20 OP2 (J), [0.6%]
S1 - DC-20 (J), [0.3%]
S1 - DG-19 (J), [0.2%]
S1 OG - DC-20 O3' (J), [0.1%]
S1 OG - DG-19 OP1 (J), [0.1%]
S1 N - DC22 O3' (I), [3.5%]
S1 OG - DC-20 O4' (J), [5.7%]
S1 OG - DG-21 N2 (J), [6.0%]
S1 - DA23 (I), [6.1%]
S1 - DC-9 (J), [0.2%]
S1 - DG-10 (J), [0.1%]
S1 - DG-8 (J), [0.4%]
S1 - DA-69 (I), [0.1%]
S1 - DC5 (I), [1.1%]
S1 OG - DC4 OP2 (I), [0.3%]
S1 - DC4 (I), [0.3%]
S1 OG - DC5 OP2 (I), [0.9%]
S1 N - DG-6 O6 (J), [1.3%]
S1 OG - DG-6 O6 (J), [0.1%]
S1 OG - DC5 N4 (I), [1.1%]
S1 N - DG-6 N7 (J), [0.1%]
S1 - DC6 (I), [0.2%]
S1 OG - DC6 OP2 (I), [0.7%]
S1 OG - DC6 O5' (I), [0.1%]
S1 - DC-11 (J), [0.6%]
S1 OG - DG-10 N7 (J), [0.1%]
G2 N - DG-19 N7 (J), [7.1%]
G2 N - DG-18 N7 (J), [3.9%]
G2 N - DG-18 O6 (J), [1.3%]
G2 N - DT-17 O4 (J), [2.1%]
G2 O - DA16 N6 (I), [1.9%]
G2 N - DT-17 OP2 (J), [0.2%]
G2 N - DG62 OP2 (J), [0.1%]
G2 N - DT12 OP1 (I), [0.1%]
G2 N - DT13 OP2 (I), [0.1%]
G2 N - DT12 OP2 (I), [0.1%]
G2 O - R69 NH2 (E), [0.4%]
G2 N - DC-20 OP1 (J), [0.1%]
G2 N - DG-19 OP1 (J), [0.1%]
G2 N - G34 O (E), [0.1%]
G2 N - DG-68 OP1 (I), [0.1%]
G2 N - DC5 OP2 (I), [0.7%]
G2 N - DC-11 OP2 (J), [0.2%]
R3 - DG-18 (J), [3.5%]
R3 - DT-17 (J), [5.3%]
R3 NH1 - DT-16 O4 (J), [0.2%]
R3 NH1 - DT14 O4 (I), [1.1%]
R3 NE - DT15 O4 (I), [0.6%]
R3 NH1 - DT15 O4 (I), [0.7%]
R3 NE - DT14 O4 (I), [0.1%]
R3 NH2 - DT15 O4 (I), [1.5%]
R3 NH2 - DT14 O4 (I), [1.4%]
R3 - DG-19 (J), [6.4%]
R3 NH1 - DT13 O4 (I), [0.3%]
R3 - DA-67 (I), [1.5%]
R3 - DG62 (J), [0.3%]
R3 - DG63 (J), [0.5%]
R3 NH2 - DT13 O4 (I), [0.3%]
R3 - DG11 (I), [1.6%]
R3 - DG-68 (I), [0.3%]
R3 - DC10 (I), [0.3%]
R3 - DT12 (I), [2.4%]
R3 - DT13 (I), [3.0%]
R3 - DT14 (I), [0.4%]
R3 NH2 - DT-16 O4 (J), [0.1%]
R3 - DC-20 (J), [10.8%]
R3 - DG-21 (J), [4.7%]
R3 NH1 - DG-21 N3 (J), [1.0%]
R3 - DG-10 (J), [3.6%]
R3 - DC-9 (J), [1.7%]
R3 - DG-8 (J), [1.1%]
R3 - DA-15 (J), [0.1%]
R3 N - G33 O (E), [0.3%]
R3 - DG-7 (J), [0.4%]
R3 NH2 - DG-7 O6 (J), [8.1%]
R3 NH1 - DG-7 N7 (J), [3.7%]
R3 NH1 - DG-7 O6 (J), [6.3%]
R3 NH2 - DG-7 N7 (J), [1.6%]
R3 NH1 - DG-6 N7 (J), [0.1%]
R3 - DC-11 (J), [1.2%]
G4 N - DT12 OP2 (I), [0.2%]
G4 N - DT12 OP1 (I), [1.0%]
G4 N - DC-20 OP2 (J), [1.5%]
G4 N - DC-20 OP1 (J), [2.1%]
G4 N - DG-21 OP2 (J), [7.4%]
G4 N - DC-9 OP2 (J), [0.9%]
K5 - DT15 (I), [0.8%]
K5 - DG-18 (J), [0.8%]
K5 - DG-19 (J), [2.3%]
K5 - DC-20 (J), [1.3%]
K5 - DG-21 (J), [0.2%]
K5 - DT12 (I), [0.4%]
K5 - DT-16 (J), [0.2%]
K5 NZ - DA-14 N7 (J), [0.1%]
K5 NZ - DT-16 O4 (J), [0.4%]
K5 - DT13 (I), [0.9%]
K5 NZ - DG-18 N7 (J), [0.1%]
K5 - DG-22 (J), [0.7%]
K5 - E73 (E), [1.8%]
K5 NZ - Q76 OE1 (E), [0.6%]
K5 NZ - N25 OD1 (F), [0.7%]
K5 N - N25 OD1 (F), [0.2%]
K5 - DC-9 (J), [2.1%]
K5 - DG-8 (J), [2.8%]
K5 - DG-10 (J), [0.2%]
K5 - DC5 (I), [0.2%]
K5 NZ - DG-7 N7 (J), [6.9%]
K5 NZ - DG-7 O6 (J), [0.4%]
K5 NZ - DG-6 O6 (J), [6.2%]
K5 NZ - DG-6 N7 (J), [0.4%]
K5 N - DG-8 N7 (J), [4.4%]
K5 O - DC7 N4 (I), [6.0%]
G6 N - DT12 OP1 (I), [0.1%]
G6 N - DT13 OP2 (I), [0.2%]
G6 N - DT13 OP1 (I), [0.4%]
G6 N - DT12 O3' (I), [0.2%]
G6 N - DC-9 OP1 (J), [1.9%]
G6 N - DC-9 OP2 (J), [2.2%]
G6 N - DG-10 OP2 (J), [0.2%]
G7 N - DT12 OP2 (I), [0.1%]
G7 N - DT12 OP1 (I), [0.5%]
G7 N - DT12 O3' (I), [0.5%]
G7 N - DT13 OP1 (I), [1.4%]
G7 N - DT13 OP2 (I), [0.2%]
G7 N - DC-9 OP2 (J), [1.3%]
G7 N - DG-8 OP2 (J), [0.1%]
K8 - DC-20 (J), [0.9%]
K8 - DG-19 (J), [1.5%]
K8 - DG-18 (J), [0.1%]
K8 - DT13 (I), [1.9%]
K8 - DT14 (I), [0.6%]
K8 - DG-21 (J), [0.2%]
K8 NZ - DT14 O4 (I), [0.2%]
K8 - DT-17 (J), [0.1%]
K8 - DT12 (I), [1.0%]
K8 - DG-8 (J), [1.0%]
K8 - DT15 (I), [0.3%]
K8 - DC-9 (J), [2.7%]
K8 - DG-10 (J), [0.8%]
K8 - DC-11 (J), [1.3%]
K8 - DC6 (I), [2.2%]
K8 - DC5 (I), [0.6%]
G9 N - DT12 OP1 (I), [0.3%]
G9 N - DT12 OP2 (I), [0.1%]
G9 N - DC-9 OP1 (J), [0.2%]
G9 N - DT13 OP1 (I), [1.6%]
G9 N - DC-9 OP2 (J), [0.2%]
G9 N - DG-10 OP1 (J), [0.1%]
L10 N - DT13 OP1 (I), [2.4%]
L10 N - DT12 O3' (I), [2.1%]
L10 N - DC-9 OP1 (J), [0.2%]
G11 N - DT13 OP1 (I), [2.1%]
K12 - DT14 (I), [0.8%]
K12 - DT13 (I), [1.0%]
K12 - DT15 (I), [1.8%]
K12 - DC-9 (J), [1.2%]
K12 - DG-10 (J), [2.9%]
K12 - DC-11 (J), [1.1%]
G13 N - DT14 OP2 (I), [0.2%]
G13 N - DT14 OP1 (I), [0.3%]
G14 N - DT14 OP1 (I), [1.6%]
K16 - DG-21 (J), [0.3%]
K16 - DG-10 (J), [0.3%]
K16 - DT14 (I), [11.5%]
K16 - DT15 (I), [1.5%]
K16 NZ - DT13 O3' (I), [0.2%]
R17 - DC-20 (J), [0.1%]
R17 - DG-19 (J), [0.1%]
R17 NH1 - DT13 O3' (I), [3.7%]
R17 - DC-11 (J), [4.2%]
R17 - DG-10 (J), [17.0%]
R17 - DT14 (I), [6.9%]
R17 NH2 - DT13 O3' (I), [0.5%]
R17 NE - DT13 O3' (I), [0.7%]
R17 NH1 - DT12 O2 (I), [0.3%]
R17 NH1 - DA-12 O3' (J), [0.3%]
H18 ND1 - DT15 OP1 (I), [2.3%]
H18 ND1 - DT15 OP2 (I), [58.6%]
R19 - DC-20 (J), [0.5%]
R19 - DG-21 (J), [1.4%]
R19 - DA16 (I), [33.5%]
R19 - DT15 (I), [3.7%]
R19 - DC-11 (J), [5.6%]
R19 - DA-12 (J), [0.4%]
R19 NH1 - DA-12 O4' (J), [0.3%]
R19 NH2 - DA-13 N3 (J), [34.2%]
R19 NH1 - DT14 O3' (I), [0.8%]
R19 NH1 - DT15 O4' (I), [0.5%]
R19 NH2 - DA-12 O4' (J), [0.2%]
R19 NH2 - DT14 O2 (I), [47.3%]
R19 NH1 - DT14 O2 (I), [0.1%]
R19 NH2 - DT14 O3' (I), [0.8%]
R19 - DG-10 (J), [0.3%]
R19 NH2 - DA-12 N3 (J), [0.1%]
R19 NH1 - DA-12 N3 (J), [0.2%]
R19 NH1 - DA-13 N3 (J), [0.1%]
R19 NH1 - DA-13 O4' (J), [4.4%]
R19 NH2 - DT15 O2 (I), [30.4%]
R19 N - DT14 O3' (I), [69.8%]
R19 NH1 - DA16 O4' (I), [3.7%]
R19 NH2 - DA-13 O4' (J), [1.0%]
R19 NE - DA-12 O4' (J), [1.9%]
R19 NH2 - DA-14 N3 (J), [0.8%]
R19 NH1 - DA-13 O3' (J), [0.3%]
K20 - DT15 (I), [4.9%]
K20 - DA16 (I), [9.5%]
K20 NZ - DT14 O3' (I), [0.1%]
R23 - DA16 (I), [44.7%]
R23 NE - Q27 OE1 (F), [0.4%]
R23 NH1 - Q27 OE1 (F), [0.6%]
R23 - DA17 (I), [2.4%]
R23 NH1 - DT15 O3' (I), [3.5%]
R23 - DA-12 (J), [48.3%]
R23 NH1 - Q27 O (F), [0.3%]
R23 NH2 - DA-13 O3' (J), [1.3%]
R23 NH2 - Q27 O (F), [0.8%]
R23 NE - Q27 O (F), [0.2%]
R23 NH1 - DA-13 O3' (J), [0.3%]
R23 - DC-11 (J), [0.1%]
D24 O - Q27 N (F), [76.3%]
D24 N - Q27 OE1 (F), [17.7%]
D24 OD2 - N25 N (F), [2.5%]
D24 O - G28 N (F), [61.9%]
D24 OD1 - N25 N (F), [2.3%]

Table S3. Annotation of the interactions shown in Figure S15 (the notations are the same as described in the legend to Table S2).

N-H4-1

S1 N - T80 OG1 (A), [0.2%]
S1 OG - DG27 OP2 (J), [1.9%]
S1 - DG27 (J), [0.3%]
S1 O - K79 NZ (B), [0.5%]
S1 OG - DG-30 OP1 (I), [1.4%]
S1 OG - DG-30 OP2 (I), [5.1%]
S1 OG - DA-31 OP1 (I), [2.6%]
S1 OG - DA-31 OP2 (I), [3.5%]
S1 - DA-31 (I), [12.4%]
S1 - DG-30 (I), [4.5%]
S1 - DC-29 (I), [4.3%]
S1 - DT-28 (I), [0.3%]
S1 OG - DC-29 OP1 (I), [0.9%]
S1 N - K77 O (B), [3.3%]
S1 - DA28 (J), [0.5%]
S1 - DC-32 (I), [0.8%]
S1 OG - DA28 OP2 (J), [0.4%]
S1 OG - K79 NZ (A), [0.5%]
S1 OG - DC-32 OP2 (I), [0.6%]
S1 OG - E74 OE2 (B), [0.5%]
S1 OG - E74 OE1 (B), [1.0%]
G2 N - DG-30 OP2 (I), [8.2%]
G2 N - DG-30 O5' (I), [1.7%]
G2 N - DA-31 OP2 (I), [0.9%]
G2 N - DA-31 OP1 (I), [0.4%]
G2 O - DC-29 N4 (I), [0.5%]
G2 N - DC-29 OP2 (I), [2.3%]
R3 N - Q76 O (A), [0.8%]
R3 - E73 (A), [4.7%]
R3 - D77 (A), [5.7%]
R3 - DA-31 (I), [21.5%]
R3 - DG-30 (I), [26.1%]
R3 - DC-32 (I), [5.7%]
R3 NE - DG-30 O6 (I), [0.7%]
R3 NH1 - DG-30 O6 (I), [2.7%]
R3 NH1 - DG29 O6 (J), [0.6%]
R3 NE - DG-30 N7 (I), [1.8%]
R3 NH2 - DG-30 O6 (I), [0.2%]
R3 NH2 - DG29 O6 (J), [0.8%]
R3 O - DC-29 N4 (I), [0.3%]
R3 - DC-29 (I), [0.4%]
G4 N - DG-30 OP2 (I), [33.0%]
G4 N - DG-30 O5' (I), [1.6%]
G4 N - DC-29 OP2 (I), [0.9%]
K5 - DC-29 (I), [19.4%]
K5 - DG-30 (I), [3.5%]
K5 - DT-28 (I), [26.5%]
K5 O - DC-27 N4 (I), [2.3%]
K5 O - DC-29 N4 (I), [0.2%]
K5 - DA-31 (I), [2.0%]
G7 N - DG27 N7 (J), [1.1%]
G7 N - DG27 O6 (J), [58.9%]
G7 N - DT-28 O4 (I), [0.6%]
G7 O - DA28 N6 (J), [0.5%]
G7 O - K79 NZ (B), [3.0%]
G7 O - DC-29 N4 (I), [2.2%]
G7 N - DG-30 OP2 (I), [0.3%]
K8 - DG27 (J), [9.3%]
K8 N - DG27 N7 (J), [2.1%]
K8 - DA28 (J), [3.7%]
K8 NZ - DA28 N7 (J), [12.9%]
K8 NZ - DG-30 O6 (I), [21.0%]
K8 NZ - DG29 O6 (J), [61.4%]
K8 NZ - DG29 N7 (J), [18.3%]
K8 NZ - DG-30 N7 (I), [1.2%]
K8 NZ - DA-31 N7 (I), [1.3%]
G9 O - T80 OG1 (A), [0.2%]
G9 O - K79 NZ (B), [2.6%]
G11 N - DG27 OP2 (J), [3.1%]
K12 - DA26 (J), [27.5%]
K12 - D81 (A), [2.8%]
K12 - DT25 (J), [0.3%]
K12 - DG27 (J), [4.8%]
G13 N - DA26 OP2 (J), [45.8%]
G13 N - DA26 OP1 (J), [2.4%]
G14 N - DT25 OP2 (J), [63.1%]
G14 N - DT25 OP1 (J), [1.4%]
A15 N - DT25 OP2 (J), [0.7%]
A15 N - DT25 OP1 (J), [2.9%]
K16 - DT25 (J), [6.2%]
K16 - DC24 (J), [25.8%]
R17 NH1 - DC-23 O3' (I), [4.4%]
R17 NE - DC-23 O3' (I), [3.6%]
R17 - DA-22 (I), [21.9%]
R17 - DA26 (J), [29.2%]
R17 - D81 (A), [29.6%]
R17 NH1 - DC-23 O4' (I), [2.1%]
R17 NH1 - DC-23 O2 (I), [4.7%]
R17 NH2 - DC-23 O2 (I), [10.1%]
R17 NH2 - DC24 O2 (J), [1.0%]
R17 NE - DA-22 N3 (I), [5.8%]
R17 NE - DA-22 O4' (I), [0.2%]
R17 NH2 - DC24 O3' (J), [0.6%]
R17 - DT25 (J), [2.0%]
R17 NH2 - DA-22 N3 (I), [9.5%]
R17 NH1 - DA-22 N3 (I), [1.6%]
R17 - DC-21 (I), [2.3%]
R17 NH1 - DC24 O3' (J), [0.8%]
R17 NH1 - DG23 O4' (J), [2.6%]
R17 NH1 - DT22 O2 (J), [2.6%]
R17 NH2 - DG23 N3 (J), [8.9%]
R17 NH2 - DG23 O4' (J), [3.1%]
R17 NH2 - DC-21 O4' (I), [1.2%]
R17 NE - DC-21 O4' (I), [0.9%]
R17 NH1 - DG23 N3 (J), [2.7%]
R17 NE - DC24 O4' (J), [1.0%]
R17 NH1 - DC24 O4' (J), [1.2%]
R17 NH2 - DT22 O2 (J), [3.3%]
H18 ND1 - DC-21 OP1 (I), [9.2%]
H18 N - DC-21 OP1 (I), [5.9%]
H18 N - DA-22 O3' (I), [5.2%]
R19 - D81 (A), [29.8%]
R19 - DA26 (J), [19.9%]
R19 - DC-21 (I), [0.5%]
R19 - DA-22 (I), [40.3%]
R19 NH1 - L82 O (A), [27.7%]
R19 NH2 - L82 O (A), [31.3%]
R19 - DC-23 (I), [2.3%]
R19 - DG27 (J), [0.2%]
R19 NH1 - DT25 O3' (J), [0.9%]
R19 NH2 - D81 O (A), [7.8%]
K20 O - Q76 NE2 (A), [4.4%]
K20 - DA-22 (I), [8.0%]
K20 - DC-21 (I), [50.9%]
K20 NZ - S10 O (A), [1.0%]
K20 NZ - S10 OG (A), [1.4%]
L22 N - Q76 OE1 (A), [30.7%]
L22 O - Q76 NE2 (A), [27.1%]
L22 O - N25 ND2 (B), [31.4%]
R23 - E73 (A), [24.4%]
R23 O - G12 N (A), [3.2%]
R23 O - S10 OG (A), [0.9%]
R23 O - T11 OG1 (A), [0.2%]
R23 O - G13 N (A), [0.8%]
R23 - D77 (A), [45.3%]
R23 O - K9 NZ (A), [1.4%]
R23 N - S10 O (A), [0.9%]
R23 NH1 - Q76 OE1 (A), [0.1%]
R23 O - K14 NZ (A), [3.3%]
D24 OD1 - G12 N (A), [2.0%]
D24 OD2 - G12 N (A), [0.8%]
D24 N - E73 OE2 (A), [46.7%]
D24 O - Q27 N (B), [74.9%]
D24 O - G28 N (B), [6.8%]
D24 OD1 - G13 N (A), [1.0%]
D24 N - E73 OE1 (A), [8.1%]
D24 OD1 - T11 OG1 (A), [0.2%]
D24 O - G13 N (A), [10.3%]
D24 OD2 - G13 N (A), [0.7%]
D24 O - Q27 NE2 (B), [0.8%]
D24 - K9 (A), [0.2%]
D24 OD2 - S10 OG (A), [0.4%]
D24 OD1 - S10 OG (A), [0.6%]
D24 - K14 (A), [0.5%]
D24 O - K14 NZ (A), [1.3%]

N-H4-2

S1 - DG-18 (J), [13.5%]
S1 OG - DG-18 OP1 (J), [4.1%]
S1 OG - DG-18 OP2 (J), [0.8%]
S1 - DG-19 (J), [1.7%]
S1 N - DC21 O2 (I), [4.6%]
S1 OG - DG-19 O3' (J), [2.4%]
S1 N - DC-20 O2 (J), [4.5%]
S1 OG - DG20 N2 (I), [1.8%]
S1 O - DG-21 N2 (J), [0.7%]
S1 OG - DG-19 OP1 (J), [0.8%]
S1 - DA24 (I), [0.3%]
S1 N - DC21 O3' (I), [5.7%]
S1 - DC22 (I), [21.5%]
S1 OG - DA23 OP1 (I), [2.5%]
S1 OG - DC21 O3' (I), [1.7%]
S1 OG - DC22 OP1 (I), [8.2%]
S1 OG - DC22 O3' (I), [0.5%]
S1 - DA23 (I), [4.9%]
S1 OG - DA23 OP2 (I), [0.7%]
S1 N - DC21 O4' (I), [0.7%]
S1 N - DG-19 N3 (J), [0.4%]
S1 OG - DG-19 N3 (J), [0.8%]
S1 O - DG20 N2 (I), [7.1%]
S1 OG - DG-19 N2 (J), [0.8%]
G2 N - DG-18 OP1 (J), [0.7%]
G2 N - DG-19 OP1 (J), [0.8%]
G2 N - DC21 O3' (I), [2.7%]
G2 N - DC22 OP1 (I), [9.2%]
G2 N - DA23 OP1 (I), [0.5%]
G2 N - DC22 O3' (I), [0.4%]
G2 N - DC21 O2 (I), [0.4%]
G2 N - DG-19 O4' (J), [3.4%]
R3 - DG-19 (J), [29.4%]
R3 - DC-20 (J), [3.0%]
R3 NH1 - DG-18 N7 (J), [0.2%]
R3 - DA23 (I), [2.6%]
R3 - DC22 (I), [2.6%]
R3 - DG-18 (J), [2.6%]
R3 NH1 - DG20 N3 (I), [2.1%]
R3 NH1 - DG-18 O4' (J), [2.4%]
R3 NH2 - DG-18 O4' (J), [1.0%]
R3 NH1 - DG20 O4' (I), [0.3%]
R3 NH1 - DC-20 O2 (J), [13.2%]
R3 NH2 - DG-19 N3 (J), [1.1%]
R3 NH1 - DG-19 N3 (J), [16.6%]
R3 NE - DG-19 N3 (J), [1.6%]
R3 NE - DG-18 O4' (J), [0.5%]
R3 NE - DG-19 O4' (J), [9.1%]
R3 NE - DC-20 O2 (J), [15.1%]
R3 NH1 - DG-19 O4' (J), [4.9%]
R3 NH2 - DC-20 O2 (J), [12.0%]
R3 NH1 - DC-20 O4' (J), [0.9%]
R3 NH2 - DG-19 O4' (J), [3.2%]
R3 NH1 - DC21 O2 (I), [1.4%]
R3 NH2 - DC-20 O4' (J), [1.4%]
R3 NH2 - DC21 O2 (I), [6.6%]
R3 NH1 - DG-21 O3' (J), [0.3%]
R3 NH2 - DG-21 N3 (J), [0.4%]
R3 NE - DC21 O3' (I), [0.4%]
R3 NH2 - DC21 O3' (I), [0.7%]
R3 NH1 - DC21 O3' (I), [0.5%]
R3 O - DG-21 N2 (J), [0.7%]
R3 NH2 - DC21 O4' (I), [2.9%]
G4 N - DG-19 OP1 (J), [2.9%]
G4 N - DG-19 OP2 (J), [1.1%]
G4 O - DG-21 N2 (J), [29.6%]
G4 N - DA23 OP1 (I), [3.1%]
G4 N - DA23 OP2 (I), [1.4%]
G4 N - DC22 O3' (I), [0.1%]
K5 - DA23 (I), [1.7%]
K5 NZ - DC22 O2 (I), [0.7%]
K5 - DG-19 (J), [13.6%]
K5 NZ - DG-21 N3 (J), [0.6%]
K5 NZ - DA23 O4' (I), [0.5%]
K5 - DA24 (I), [5.8%]
K5 - DG25 (I), [0.5%]
K5 N - DC-20 O3' (J), [0.6%]
K5 NZ - DA24 O4' (I), [2.7%]
K5 NZ - DA23 N3 (I), [5.5%]
K5 NZ - DA24 N3 (I), [1.2%]
G6 N - DC-20 OP1 (J), [0.1%]
G6 N - DG-19 OP1 (J), [1.6%]
G6 N - DC-20 O3' (J), [0.7%]
G6 O - DG-22 N2 (J), [54.2%]
G6 N - DA23 OP1 (I), [3.5%]
G6 N - DA23 O5' (I), [0.8%]
G6 N - DC22 O2 (I), [11.5%]
G7 N - DG-21 O3' (J), [1.0%]
G7 N - DC-20 OP1 (J), [0.3%]
G7 N - DG-21 O4' (J), [62.9%]
G7 N - DA23 O3' (I), [2.8%]
G7 N - DA24 OP1 (I), [1.7%]
K8 - DG-21 (J), [1.8%]
K8 NZ - DA23 O3' (I), [0.1%]
K8 - DA24 (I), [0.3%]
K8 - DG25 (I), [5.4%]
K8 NZ - DT-23 O2 (J), [21.4%]
K8 NZ - DA24 N3 (I), [12.0%]
K8 - DG-22 (J), [14.0%]
K8 N - DA23 N3 (I), [0.7%]
K8 NZ - DT-23 O3' (J), [5.7%]
K8 N - DG-22 O4' (J), [1.6%]
K8 - DG26 (I), [15.1%]
G9 N - DG-21 OP1 (J), [0.4%]
L10 N - DG25 OP1 (I), [17.4%]
L10 N - DA24 O3' (I), [36.1%]
L10 N - DG-21 OP1 (J), [0.4%]
G11 N - DG-21 OP1 (J), [3.8%]
G11 N - DG-22 O3' (J), [3.0%]
G11 N - DG25 OP1 (I), [28.9%]
G11 N - DA24 O3' (I), [0.9%]
K12 - DG25 (I), [3.0%]
K12 - DG26 (I), [3.6%]
K12 - DC-20 (J), [23.1%]
K12 - DG-21 (J), [0.5%]
K12 - DG-22 (J), [1.8%]
K12 - DG27 (I), [0.3%]
K12 - D81 (E), [0.9%]
G13 N - DG-21 OP1 (J), [0.3%]
G13 O - R83 NH2 (E), [1.2%]
G13 O - K79 NZ (F), [0.1%]
G13 N - DG26 OP1 (I), [1.1%]
G14 N - DG27 OP1 (I), [2.9%]
G14 O - R83 NH2 (E), [2.0%]
G14 O - R83 NE (E), [2.1%]
G14 N - DG-21 OP1 (J), [1.0%]
A15 N - D81 OD2 (E), [2.5%]
A15 N - D81 OD1 (E), [4.3%]
A15 O - Q76 NE2 (E), [3.5%]
A15 N - L82 O (E), [0.3%]
A15 O - R72 NH2 (E), [1.0%]
A15 N - DT-23 O3' (J), [2.1%]
A15 N - DG-21 OP1 (J), [34.7%]
A15 N - DC-20 OP2 (J), [0.8%]
K16 - DC-20 (J), [6.2%]
K16 - DG-21 (J), [20.8%]
K16 - DG-22 (J), [8.1%]
K16 - D81 (E), [4.5%]
K16 O - R72 NH2 (E), [0.4%]
K16 - E73 (E), [0.1%]
R17 - DG-22 (J), [7.5%]
R17 - D81 (E), [7.9%]
R17 O - N25 ND2 (F), [3.2%]
R17 - E73 (E), [28.3%]
R17 - D77 (E), [13.4%]
R17 NH1 - E73 O (E), [1.1%]
R17 NH2 - Q76 OE1 (E), [0.4%]
R17 - DG-21 (J), [2.9%]
R17 - DC-20 (J), [1.3%]
H18 NE2 - N25 ND2 (F), [5.0%]
H18 ND1 - E73 OE2 (E), [0.5%]
H18 ND1 - E73 OE1 (E), [0.5%]
H18 ND1 - N25 OD1 (F), [0.3%]
H18 NE2 - R72 NH1 (E), [0.5%]
H18 NE2 - R72 NH2 (E), [0.2%]
R19 - DC-20 (J), [7.3%]
R19 O - R69 NH2 (E), [11.5%]
R19 - DG-21 (J), [16.3%]
R19 O - R69 NE (E), [5.5%]
R19 - DG-22 (J), [33.0%]
R19 NH1 - DG-19 O6 (J), [9.5%]
R19 NH1 - DG-19 N7 (J), [31.6%]
R19 NH2 - DG-19 N7 (J), [0.5%]
R19 NH2 - DG-19 O6 (J), [38.0%]
R19 NH1 - DG-18 O6 (J), [1.7%]
K20 - DA16 (I), [15.2%]
K20 - DA17 (I), [5.8%]
K20 - DC-20 (J), [1.4%]
K20 - DG-21 (J), [0.8%]
K20 NZ - DA17 N7 (I), [4.2%]
K20 NZ - DG-19 N7 (J), [1.7%]
K20 NZ - DG-19 O6 (J), [1.5%]
K20 NZ - DG-18 O6 (J), [1.4%]
K20 NZ - DA16 N7 (I), [2.9%]
K20 NZ - DT-17 O4 (J), [0.4%]
V21 O - N25 ND2 (F), [0.5%]
L22 O - N25 ND2 (F), [2.6%]
L22 N - N25 OD1 (F), [2.3%]
L22 N - DA16 OP1 (I), [6.4%]
L22 N - DA16 OP2 (I), [14.8%]
R23 NH1 - Q27 OE1 (F), [1.7%]
R23 NE - Q27 OE1 (F), [2.2%]
R23 O - N25 N (F), [2.0%]
R23 O - N25 ND2 (F), [1.0%]
R23 NH1 - Q27 O (F), [0.6%]
R23 - DA-12 (J), [59.7%]
R23 - E73 (E), [0.2%]
R23 - DA16 (I), [62.5%]
R23 NH1 - DT15 O3' (I), [46.6%]
R23 NH1 - DA-13 O3' (J), [1.3%]
R23 NH2 - Q27 O (F), [3.3%]
R23 NH2 - DA-13 O3' (J), [10.7%]
R23 NH2 - DT15 O3' (I), [0.5%]
D24 N - Q27 OE1 (F), [10.6%]
D24 OD2 - N25 N (F), [9.2%]
D24 OD1 - N25 N (F), [8.5%]
D24 OD1 - I26 N (F), [2.6%]
D24 O - Q27 N (F), [70.6%]
D24 O - G28 N (F), [51.3%]
D24 OD2 - I26 N (F), [2.8%]
D24 OD2 - Q27 N (F), [0.9%]

Figures

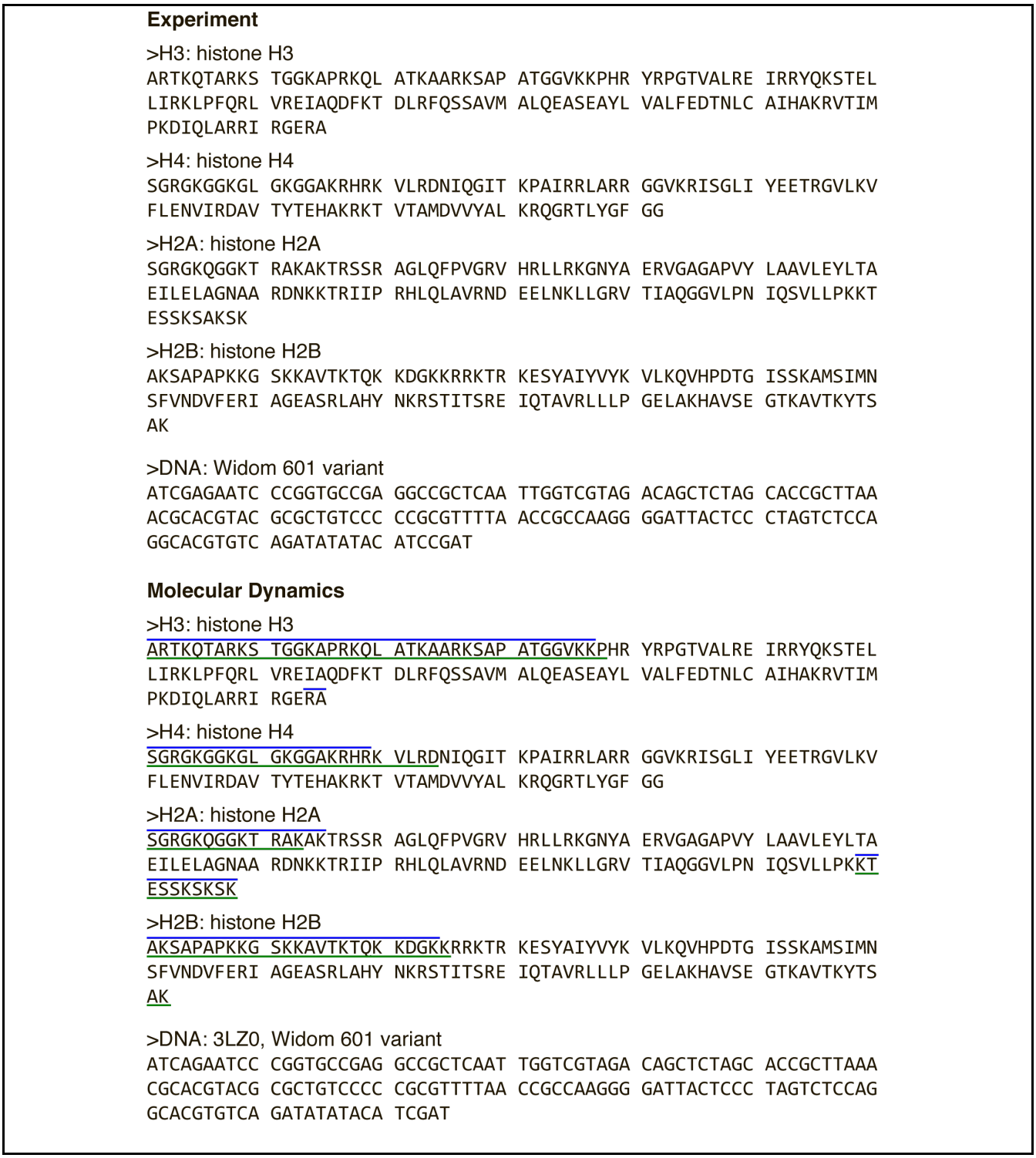

Figure S1. Sequences of histones and DNA used in the NMR experiments and MD simulations. In generating the 3LZ0-based models for MD simulations, the histone tails were rebuilt as indicated by blue overline and green underline (corresponding to the first and second copy of histone protein, respectively). The DNA sequence used in the simulations is numbered from -72 to 72; the experimental sequence contains two additional nucleotides inserted between positions -70 and -69 and between positions 68 and 69. The histone sequences in the MD model are identical to the ones employed in the experiment, with the exception of residue A126 in H2A that is absent from the model.

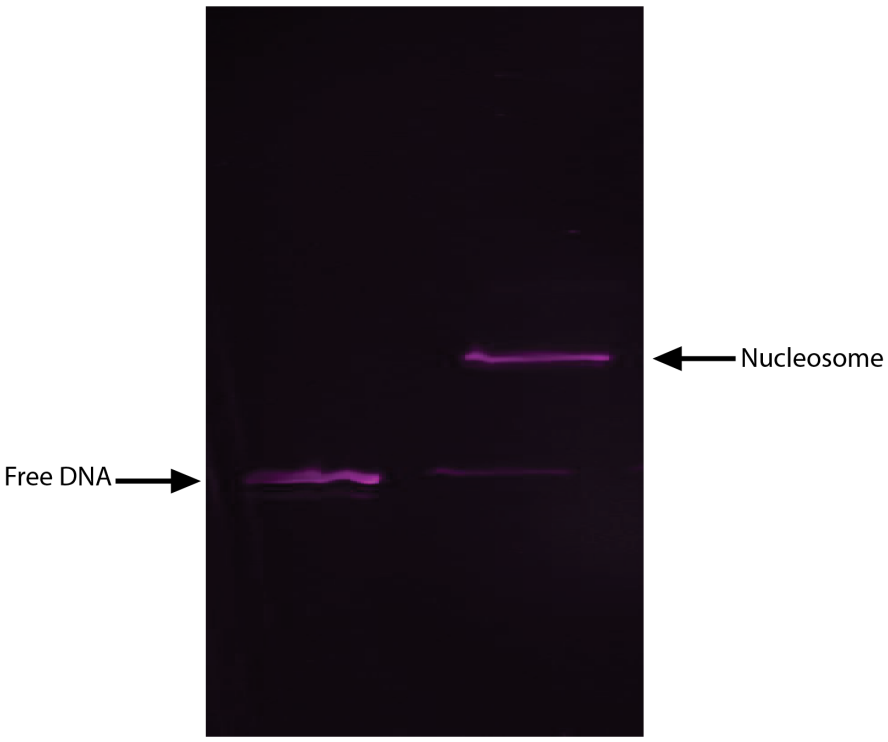

Figure S2. Native acrylamide gel (5%) showing the shift in electrophoretic mobility between 147 bp Widom 601 DNA and mononucleosomes. Left lane: 147 bp DNA; Right lane: Sucrose gradient purified mononucleosomes (300 ng) prepared as described in the Methods section and used for the NMR measurements.

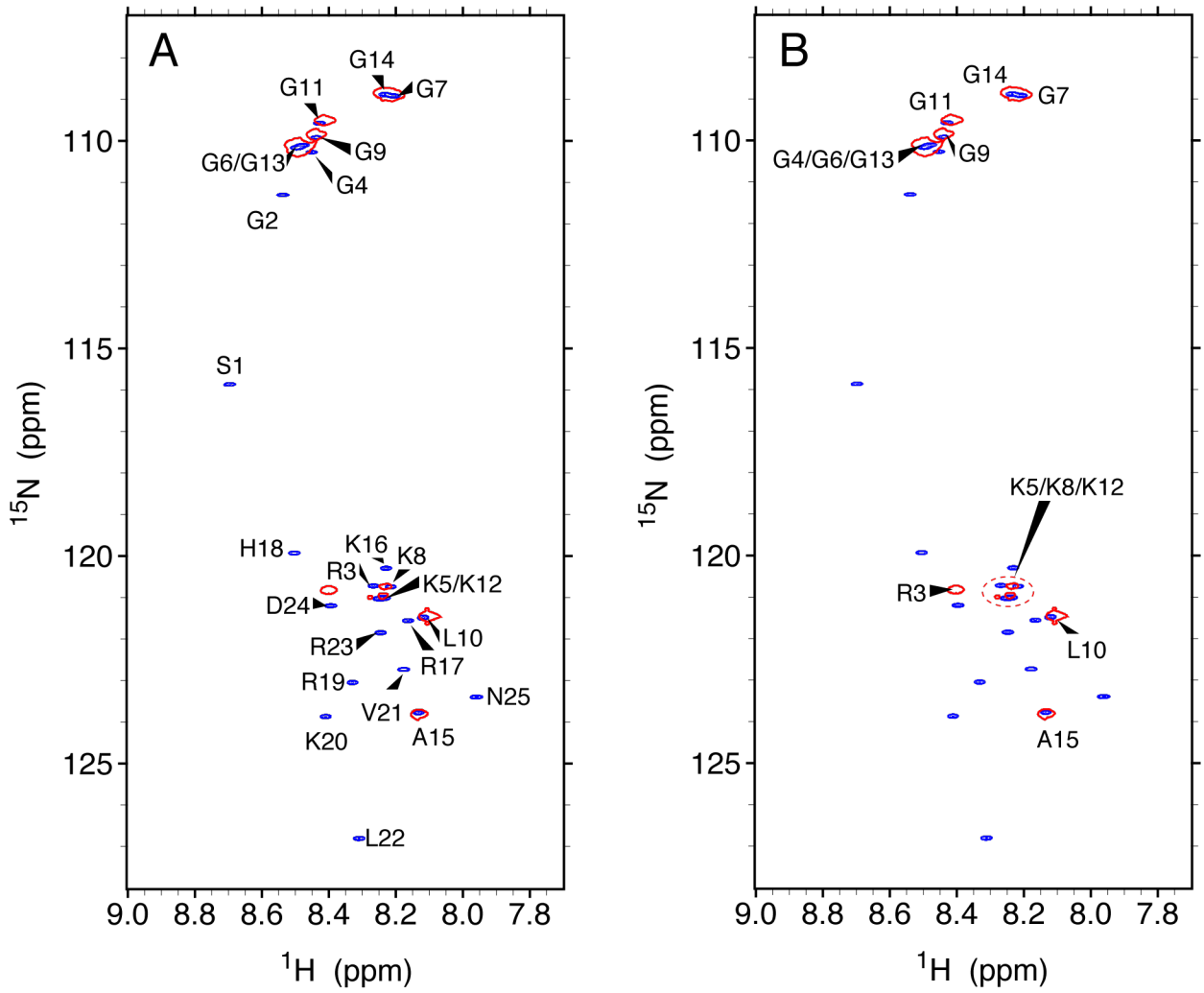

Figure S3. The superposition of $^{1}H^{N}$,^{15}N-HSQC spectra from NCP sample containing ^{15}N-labeled H4 histone proteins (red) and for 26-aa N-H4 peptide GSGRGKGGKGLGKGGAKRHRKVLRDN[26] (blue). Panel (A) shows the free peptide assignment, while panel (B) shows the NCP assignment. The peak positions in the NCP spectrum are near identical to those in the peptide spectrum. The sole exception is the resonance R3, where a small downfield shift in proton dimension is observed.

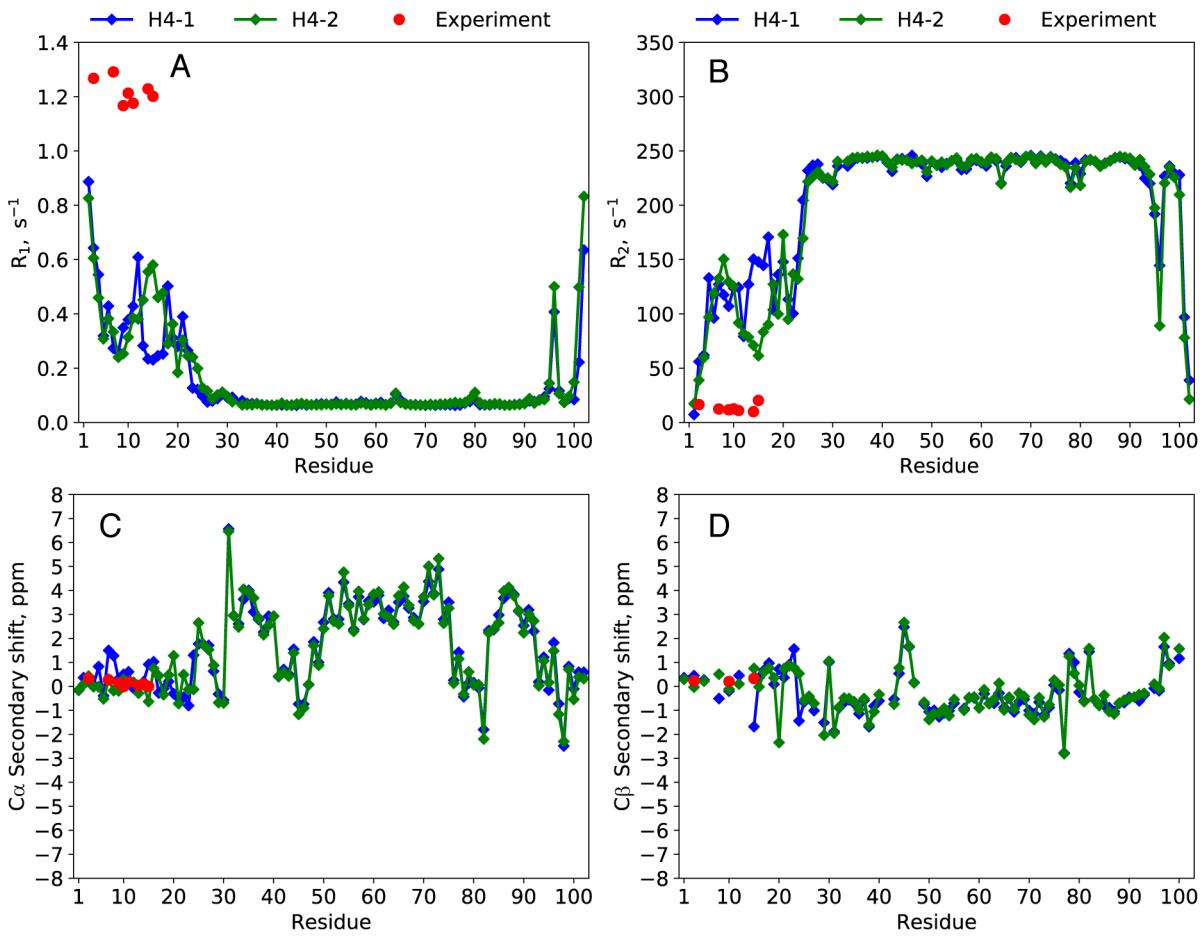

Figure S4. (A, B) ^{15}N relaxation rate constants R_1, R_2 and (C, D) ^{13}C secondary chemical shifts δ_{sec} for H4 histone proteins in NCP. Experimental values are shown with red circles, the results of MD-based calculations – with blue and green diamonds (first and second copy of H4, as enumerated in the structure 3LZ0). The MD trajectory is that of NCP in TIP3P water, with net length of 1 μs.

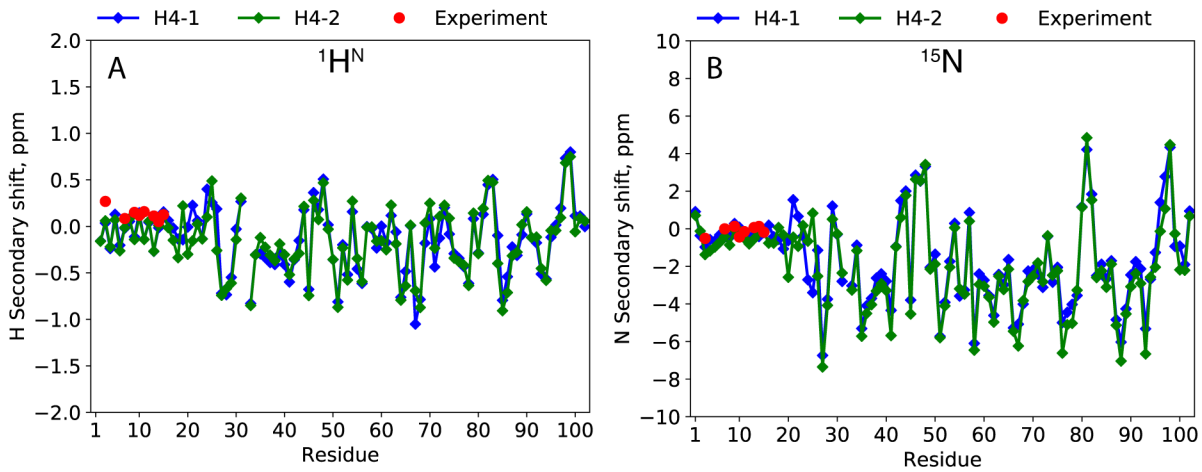

Figure S5. (A) $^1H^N$ and (B) ^{15}N secondary chemical shifts δ_{sec} for H4 histone proteins in NCP. Experimental values are shown with red circles, the results of MD-based calculations – with blue and green diamonds (first and second copy of H4, as enumerated in the structure 3LZ0). The MD trajectory is that of NCP in TIP4P-D water, with net length of 2 μs.

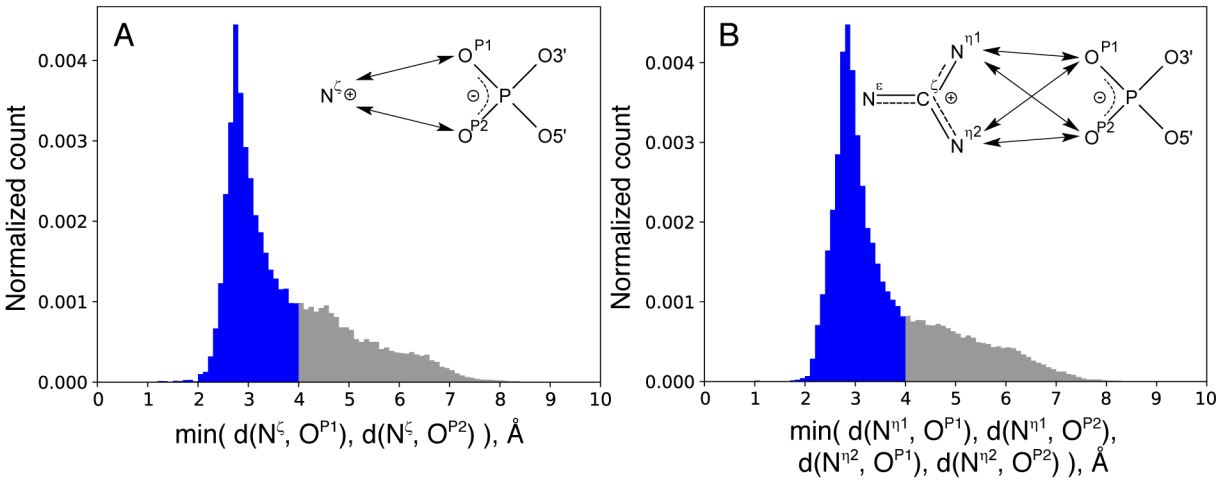

Figure S6. While there has been discussion of salt bridges between DNA phosphates and basic side chains in the literature,[27] there is no commonly accepted structural criterion for identification of such salt bridges. To look into this problem, we have analyzed a set of 4,810 PDB structures of protein-DNA complexes with crystallographic resolution better than 3.5 Å. From this dataset, we have extracted 42,705 lysine-phosphate pairs, 1,826 (N-terminus)-phosphate pairs and 55,623 arginine-phosphate pairs with separation of less than 8.0 Å between one of the nitrogen atoms (N$^{\zeta}$, terminal N, N$^{\eta1}$ or N$^{\eta2}$) and phosphorus atom P. These data were histogrammed as a function of a minimal nitrogen-to-oxygen distance for (A) lysine-phosphate and (B) arginine-phosphate pairs. Only OP1 and OP2 atoms have been taken into consideration, but not O3' or O5' (see insets). The probability density was normalized according to the slice volume $4\pi r^2 dr$. The obtained distributions feature pronounced maxima at 2.7-2.9 Å. The inspection of the distributions leads to the following operational definitions of salt bridges: min(d(N$^{\zeta}$, O^{P1}), d(N$^{\zeta}$, O^{P2})) < 4.0 Å for lysine-phosphate bridge and min(d(N$^{\eta1}$, O^{P1}), d(N$^{\eta1}$, O^{P2}), d(N$^{\eta2}$, O^{P1}), d(N$^{\eta2}$, O^{P2})) < 4.0 Å for arginine-phosphate bridge. This definition is analogous to the one commonly used for protein salt bridges.[28] Given the relatively small sample of (N-terminus)-phosphate bridges, we propose to treat them in the same manner as lysines. As mentioned above, oxygen atoms O3' or O5' are not included in the definition of salt bridges although they bear significant negative charges. The distribution of distances between N$^{\zeta}$, N$^{\eta1}$ or N$^{\eta2}$ and either O3' or O5' does not show any sharp bell-type feature such as seen in this graph and actually peaks at around 5 Å, suggesting that these pairs do not contribute to the salt-bridge interactions.

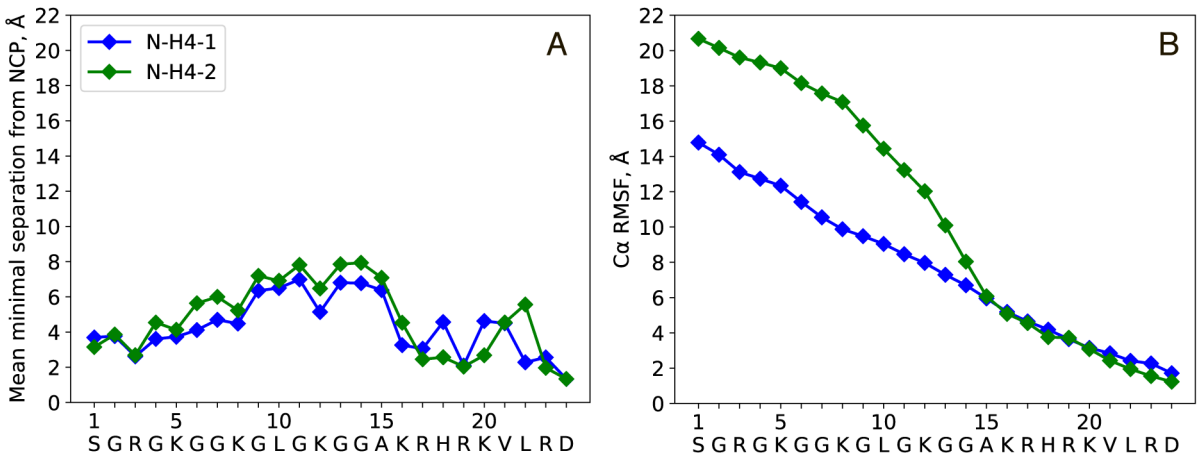

Figure S7. (A) Separation between N-H4 tails and the rest of the NCP. Calculated as a minimal atom-to-atom distance using individual frames in the (Amber ff14SB / TIP4P-D) trajectory and then frame-averaged. (B) Root mean square fluctuations (rmsf) of N-H4 C^{α} atoms. Although N-H4-1 and N-H4-2 maintain close contact with the body of NCP, they are also widely spread over the nucleosomal surface. Despite the fact that residue R3 in N-H4-1 remains anchored for nearly two-thirds of the trajectory, the corresponding C^{α} rmsf value is substantial, 13.1 Å; this is due to the fuzzy dynamics of N-H4-1 during the initial one-third of the simulation, when R3 visits a number of different sites on the surface of NCP. For the more mobile tail, N-H4-2, the 1-15 segment sweeps a wide swath of the NCP surface, resulting in a C^{α} rmsf value of 19.6 Å for residue R3.

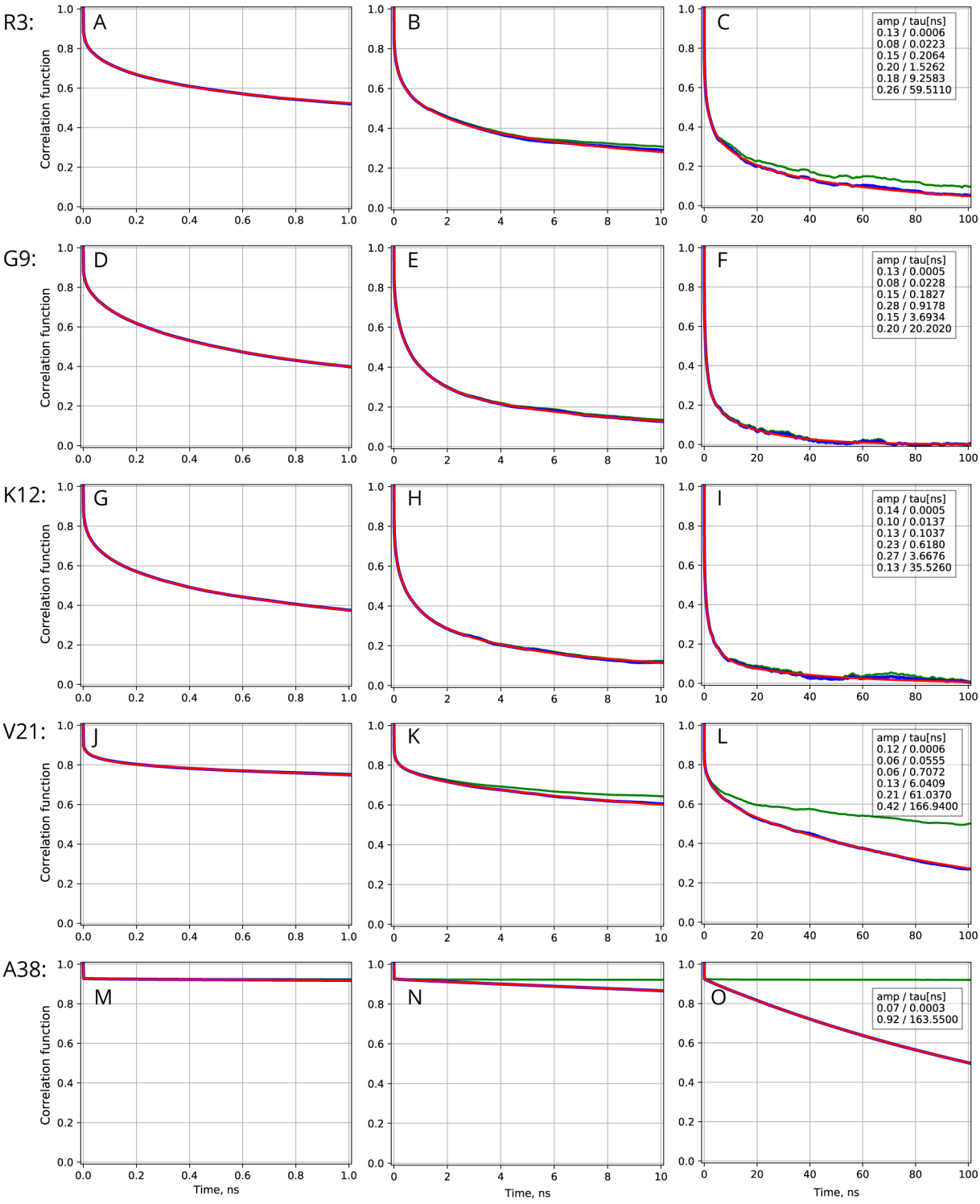

Figure S8. Reorientational correlation functions $C_{NH}(t)$ for residues R3, G9, K12, V21 and A38 in H4-2 histone protein as calculated from 2-μs (Amber ff14SB / TIP4P-D) trajectory of NCP. For each residue, the same set of curves is plotted from 0 to 1 ns (left panel), 0 to 10 ns (middle panel) and 0 to 100 ns (right panel). The trajectory was first post-processed to eliminate the overall tumbling of the NCP and the correlation functions representative of internal dynamics have been computed (green curves). Then the overall tumbling was reintroduced by multiplying the result by $exp(-\tau/\tau_{rot})$, where τ_{rot} is 163.4 ns (blue curve). Finally, we fit the result with a six-exponential fitting function (red curve). The outcome of the fitting procedure, i.e. a set of unconstrained weights and correlation times, is reported in the rightmost panels (those components whose weight is less than 0.01 are not listed). The fitting was found to be stable and fully reproducible.

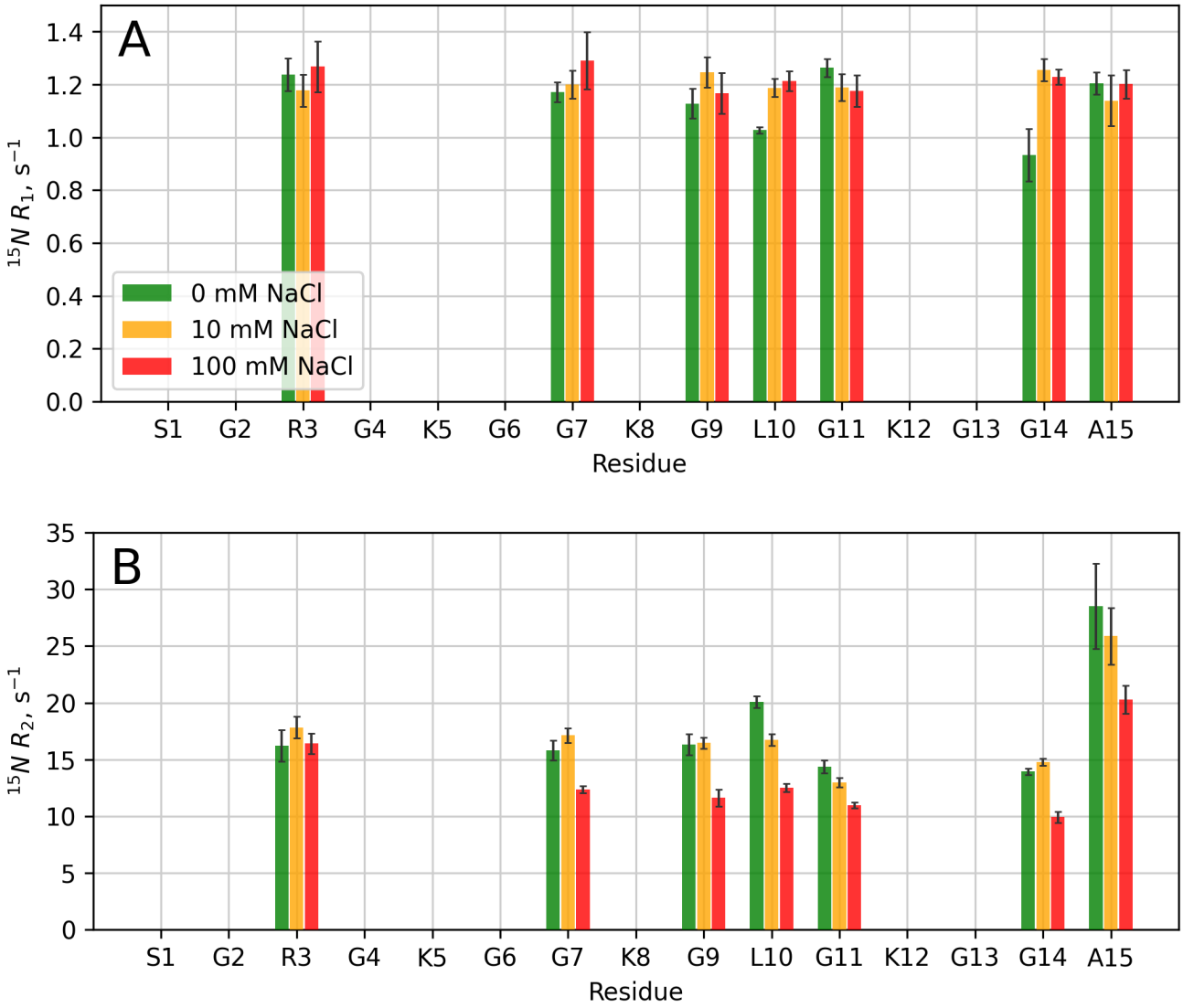

Figure S9. ^{15}N relaxation rate constants (A) R_1 and (B) R_2 for N-H4 tails of NCP. The rates have been measured in solution with different ionic strength: 0, 10 and 100 mM NaCl (green, yellow and red bars, respectively). Note that R_2 is a convenient measure of local dynamics: increased mobility (i.e., greater motional amplitudes and shorter correlation times) leads to lower relaxation rates. In contrast, longitudinal spin relaxation rate R_1 has a complex dependence on local motions[29] and, therefore, is ill-suited to detect small changes in N-H4 dynamics.

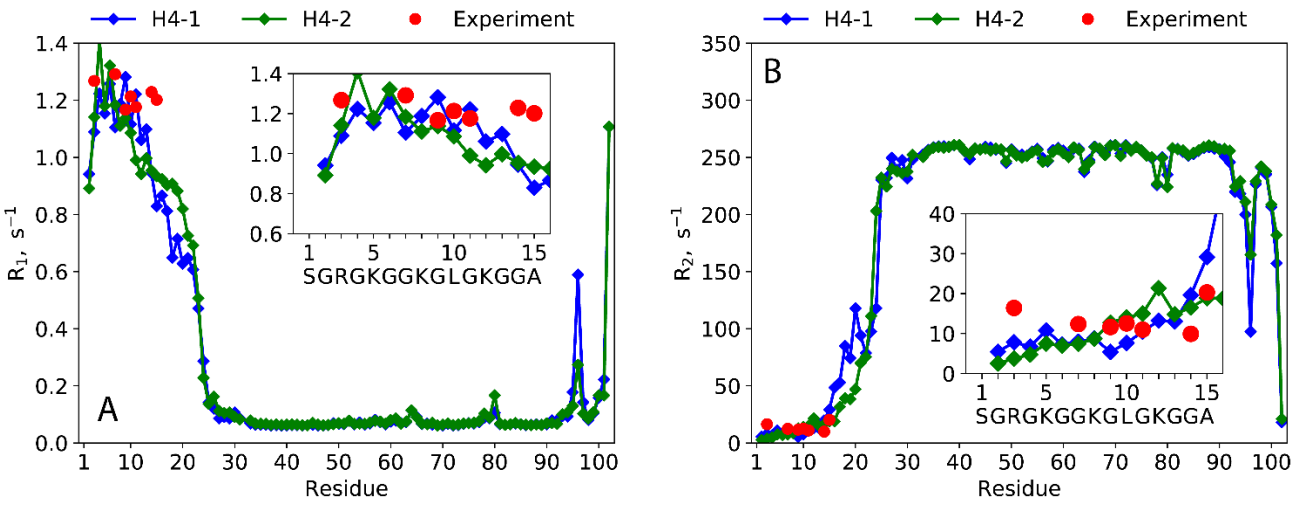

Figure S10. ^{15}N relaxation rate constants (A) R_1 and (B) R_2 for H4 histone proteins in NCP. Experimental values, shown with red circles, are the same as in Figure 2. The results of MD-based calculations are from 1.35 μs (Amber ff14SB / TIP4P-D) trajectory of NCP at high salt concentration, 0.8 M NaCl. While it is known that NCPs dissociate at this ionic strength,[30] the dissociation occurs on a much longer time scale than the length of our simulations.[31] In the current 1.35 μs MD trajectory the structure of NCP remains essentially intact, see Figure S13. Therefore, this trajectory can be seen as a reasonable *in silico* model to characterize the effect of high ionic strength on the mobility of H4 tails. Comparing the results in this figure with those in Figure 2, we conclude that high salt concentration scales down the electrostatic interactions between N-H4 and nDNA and thereby makes N-H4 more dynamic.

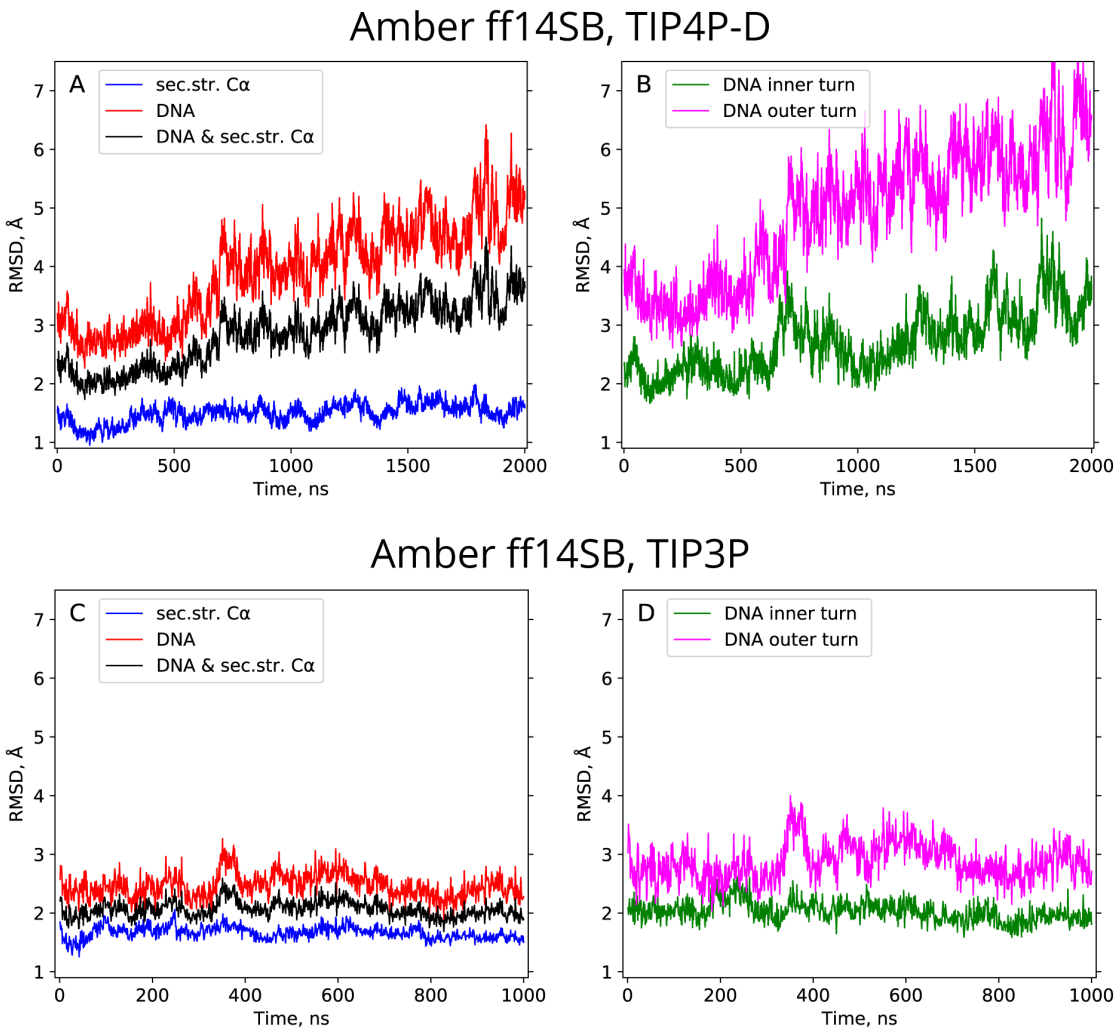

Figure S11. (A,B) Rmsd traces for 2-μs (Amber ff14SB / TIP4P-D) trajectory of NCP. All frames in the trajectory have been superimposed onto the reference structure PDB ID 3LZ0, using for this purpose only C^{α} atoms from the rigid histone scaffold (i.e. those C^{α} atoms that belong to the α-helical secondary structure in the coordinate set 3LZ0). Subsequently, rmsd values have been calculated using different sets of atoms: (i) the same C^{α} atoms that have been used to overlay the frames (blue curve); (ii) N1 and N9 atoms from nDNA nucleobases[32] (red curve); (iii) sets (i) and (ii) combined (black curve); (iv) N1 and N9 atoms from the inner turn of nDNA, nucleotides from -38 to 38 (green curve); (v) N1 and N9 atoms from the outer turn of nDNA, nucleotides from -72 to -39 and from 39 to 72 (magenta curve). The sampling step is 1 ns. (C,D) Rmsd traces representative of 1-μs (Amber ff14SB / TIP3P) trajectory of NCP. Same computational protocol and graphing conventions are used as in panels (A,B).

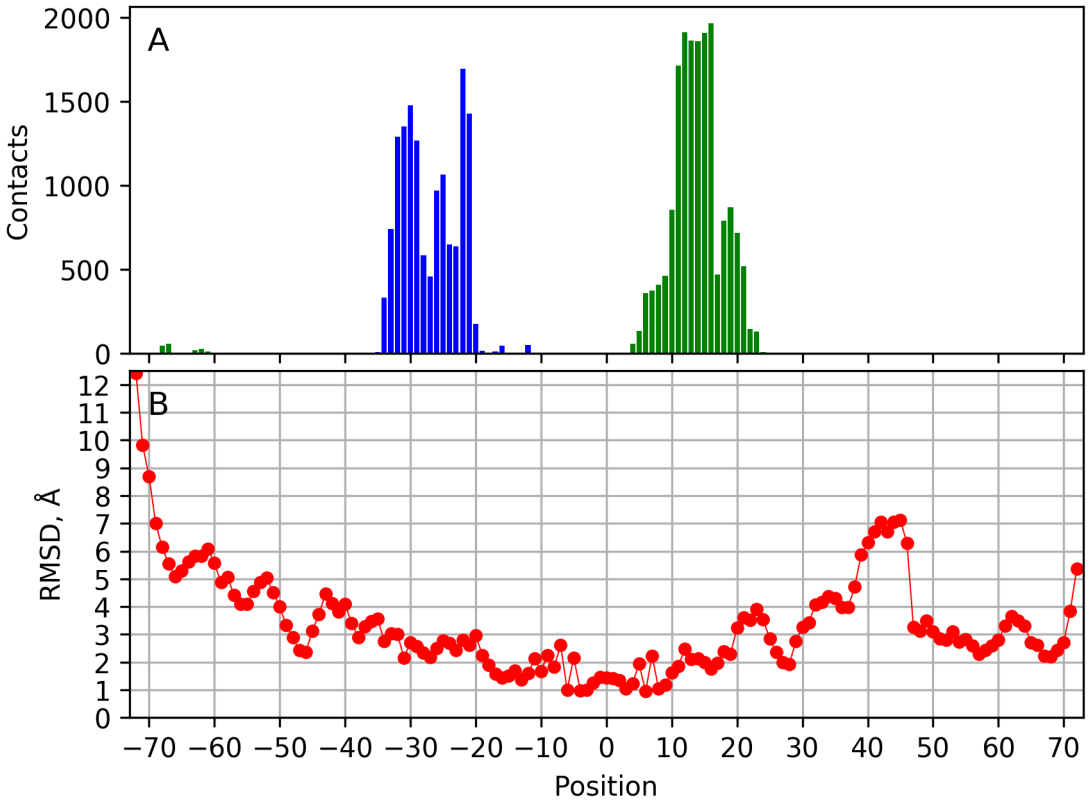

Figure S12. (A) The occurrence of contacts between N-H4 tails and nDNA base pairs in 2-μs (Amber ff14SB / TIP4P-D) simulation. Base-pair numbers are indicated underneath panel B. It is assumed that the contact occurs when one of the heavy atoms in the N-H4 tail is within 4 Å from one of the heavy atoms in the individual base pair. The histograms for N-H4-1 and N-H4-2 contacts are plotted using blue and green bars, respectively. (B) Mean rmsd values for the individual base pairs in nDNA. The procedure to align frames is the same as described in the caption of Figure S11; the base-pair-specific rmsd involves two N1 atoms and one N9 atom. The results are averaged over the entire length of the trajectory. The results suggest that the N-H4 tails interact mainly with the inner turn of nDNA and thus should have little influence on the unwrapping of the outer turn, unlike N-H3 tails that are known to stabilize the outer turn.[33] To further illustrate this point, we have calculated the rmsd characteristic only of those nucleotides that are in contact with N-H4 tails. Specifically, each frame was scanned to identify such contacts – and the current coordinates of the involved nucleotides have been included in the calculation of rmsd. The resulting rmsd values were 2.8 Å for N-H4-1 and 2.2 Å for N-H4-2 (this result is similar to what is seen in the TIP3P trajectory, see Figure S11C).

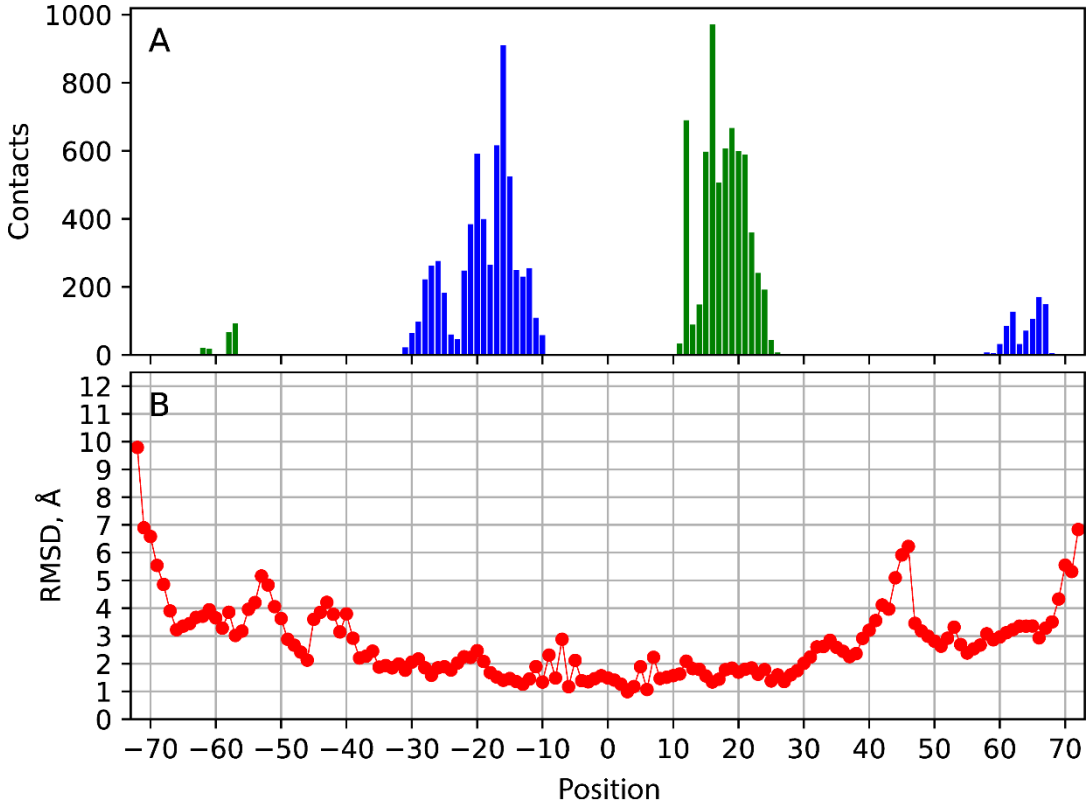

Figure S13. (A) The occurrence of contacts between N-H4 tails and nDNA base pairs in 1.35-μs (Amber ff14SB / TIP4P-D) simulation with 800 mM NaCl and (B) mean rmsd values characterizing displacement of the nDNA base pairs relative to the reference structure 3LZ0 (see caption of Figure S12 for details of calculations). Interestingly, the rmsd profile reproduces certain features that have been observed under low-salt conditions, e.g. elevated values around b.p. 45, cf. Figure S12.

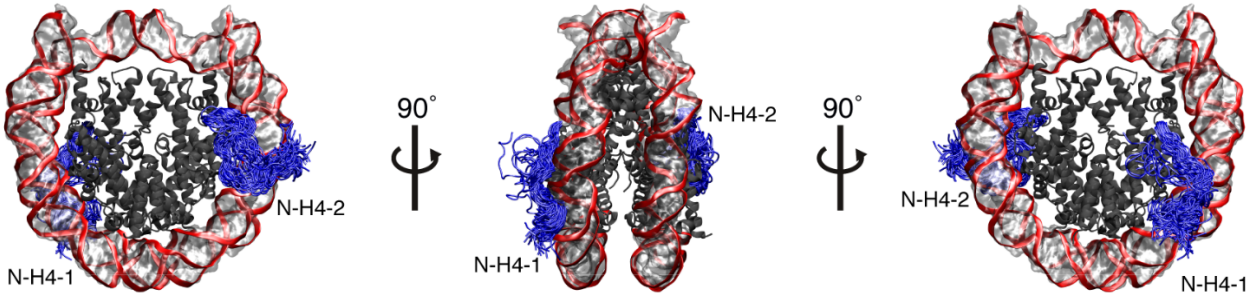

Figure S14. Dynamics of N-H4 tails in 1-μs (Amber ff14SB / TIP3P) simulation. To generate this plot, the trajectory was sampled with the step of 10 ns; the extracted frames were overlaid onto the reference structure 3LZ0 (superimposed via the secondary-structure C^{α} atoms from the histone core). The plotting conventions are the same as in Figure 1B. The radius of gyration calculated for this trajectory is R_g = 42.0 ± 1.0 Å, which is lower than the experimentally determined value 43.7 Å.

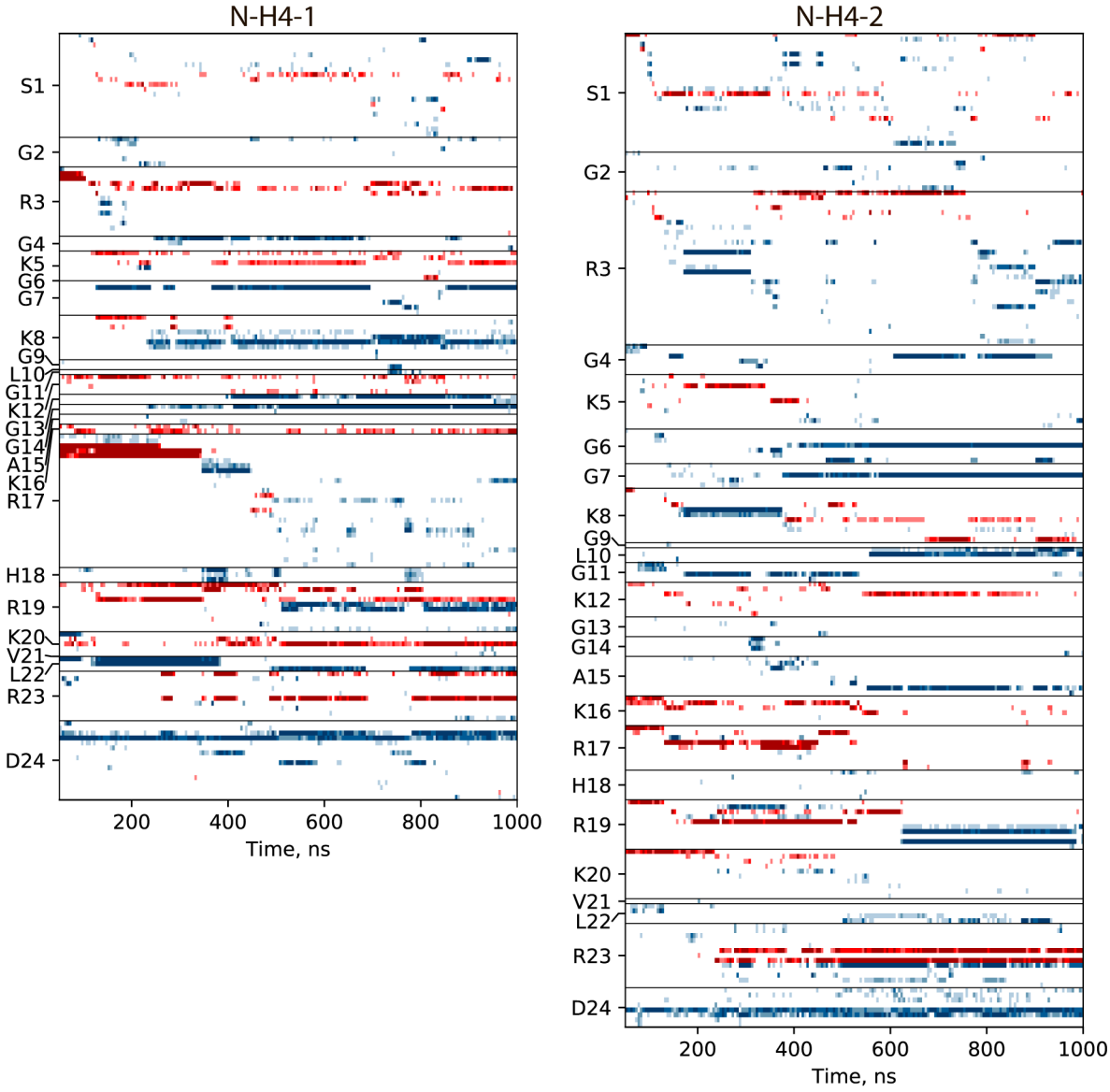

Figure S15. Traces of interactions between N-terminal tails of H4 histones and the remaining part of the NCP as observed in the 1-μs (Amber ff14SB / TIP3P) trajectory. The plotting format is the same as in Figure 3 (including the width of the colored bands). The ordered list of all interactions can be found in Table S3. The proportion of persistent interactions in the (Amber ff14SB / TIP3P) model is significantly higher than that in the (Amber ff14SB / TIP4P-D) model.

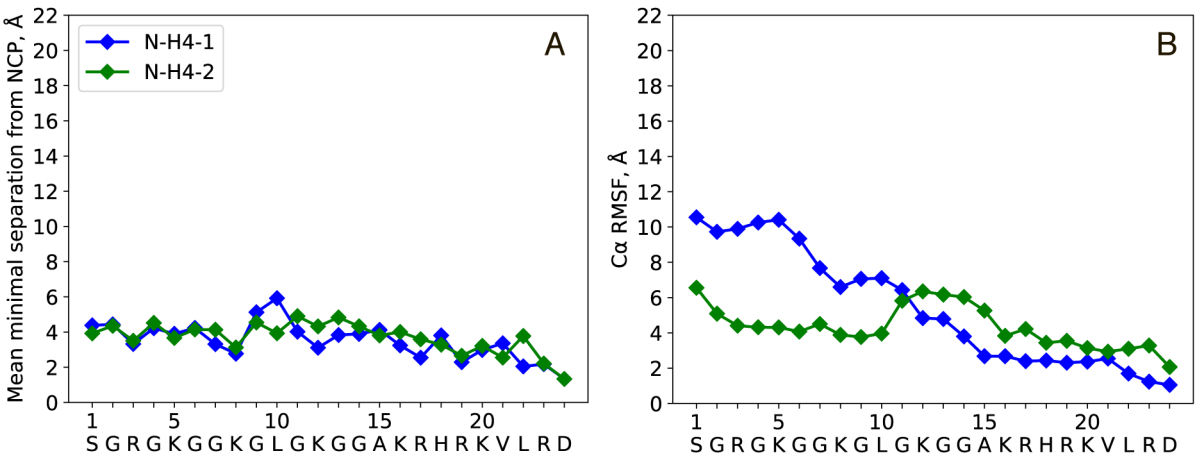

Figure S16. (A) Separation between N-H4 tail and the rest of NCP and (B) root mean square fluctuations (rmsf) of N-H4 C^{α} atoms as found in 1-μs (Amber ff14SB / TIP3P) simulation.

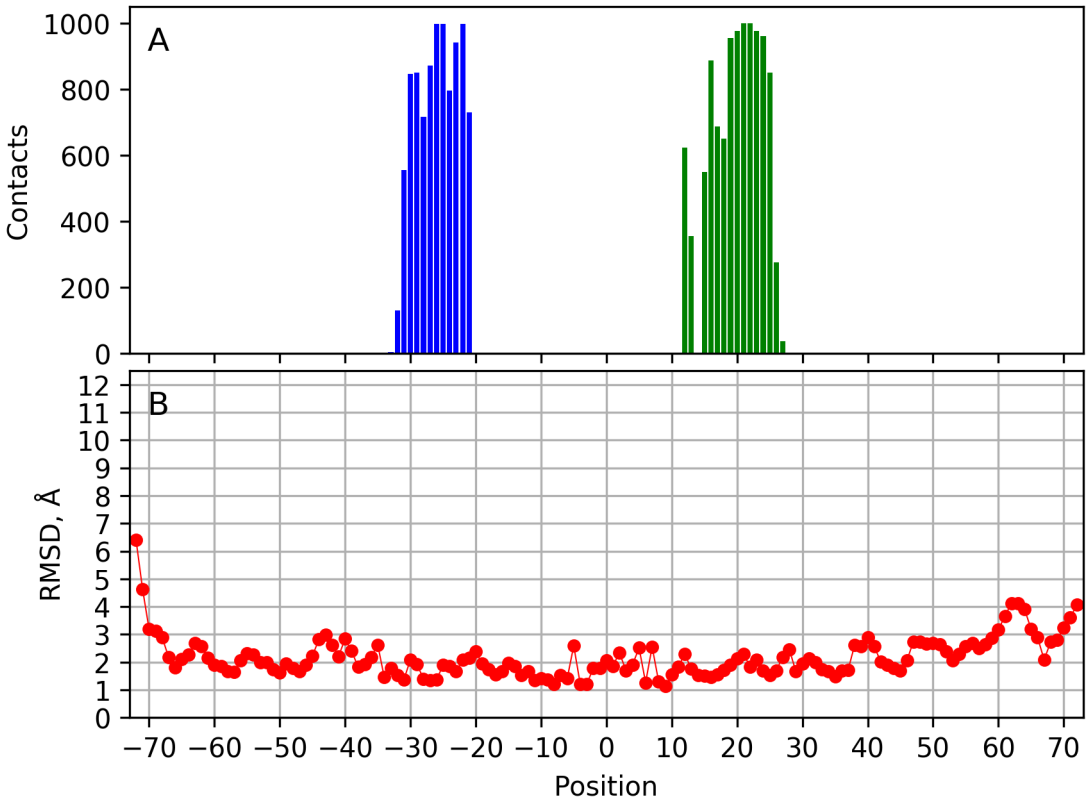

Figure S17. (A) The occurrence of contacts between N-H4 tails and nDNA base pairs in (Amber ff14SB / TIP3P) simulation and (B) mean rmsd values characterizing displacement of the nDNA base pairs relative to the reference structure 3LZ0. See caption of Figure S12 for details of the calculations. Interestingly, several base pairs at the 5' end of the template strand show a tendency to disengage from the body of the NCP. Somewhat elevated rmsd is also observed for a dozen of base pairs at the 3' end, which may tentatively reflect the tendency of nDNA to unwrap beginning from this end.[34]

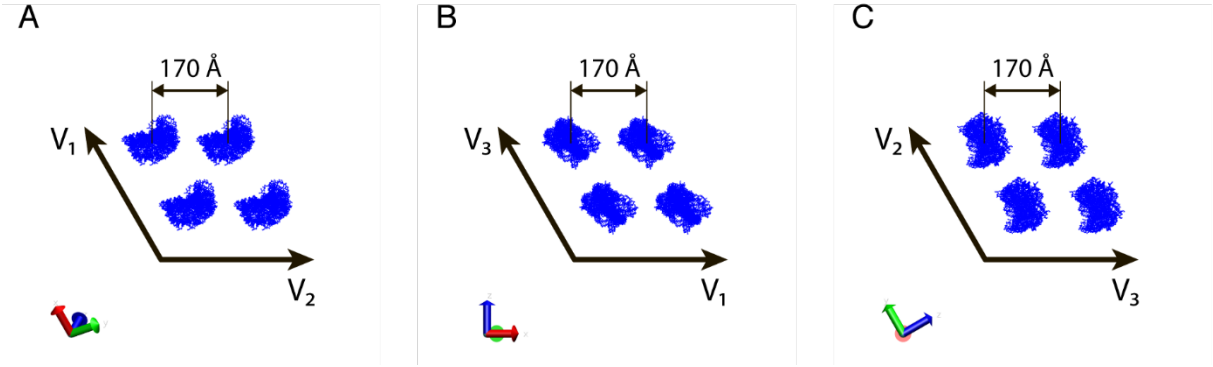

Figure S18. NCP and its periodic images in the first frame of the (Amber ff14SB / TIP4P-D) trajectory (following resolvation into a smaller box). Shown are the three planar projections of the periodic image lattice, which is defined by the plane translation vectors $\overrightarrow{V_1}$, $\overrightarrow{V_2}$ and $\overrightarrow{V_3}$ (making the angle of 109.47° with each other). The PDB frame is shown with colored arrows.

Animations

Movie S1. Animations showing dynamics of N-H4 tails in the (A) 1-μs (Amber ff14SB / TIP3P) trajectory and (B) 2-μs (Amber ff14SB / TIP4P-D) trajectory of NCP. The DNA backbone is shown as a red band, bases and sugars are shown as a semi-transparent surface, the bodies of histone proteins are grey, the N-H4 tails are cyan (labeled in the plot) and other histone tails are not shown.

References

[1] a) P. N. Dyer, R. S. Edayathumangalam, C. L. White, Y. H. Bao, S. Chakravarthy, U. M. Muthurajan, K. Luger, in *Chromatin and Chromatin Remodeling Enzymes, Pt A, Vol. 375* (Eds.: C. D. Allis, C. Wu), Elsevier Academic Press Inc, San Diego, **2004**, pp. 23-44; b) E. A. Morrison, J. C. Sanchez, J. L. Ronan, D. P. Farrell, K. Varzavand, J. K. Johnson, B. X. Gu, G. R. Crabtree, C. A. Musselman, *Nat. Commun.* **2017**, *8*, 16080.

[2] M. Sattler, J. Schleucher, C. Griesinger, *Prog. NMR Spectrosc.* **1999**, *34*, 93-158.

[3] a) N. A. Lakomek, J. F. Ying, A. Bax, *J. Biomol. NMR* **2012**, *53*, 209-221; b) M. Gairi, A. Dyachenko, M. T. Gonzalez, M. Feliz, M. Pons, E. Giralt, *J. Biomol. NMR* **2015**, *62*, 209-220.

[4] M. Tollinger, N. R. Skrynnikov, F. A. A. Mulder, J. D. Forman-Kay, L. E. Kay, *J. Am. Chem. Soc.* **2001**, *123*, 11341-11352.

[5] J. L. Kiteyski-LeBlanc, T. Yuwen, P. N. Dyer, J. Rudolph, K. Luger, L. E. Kay, *J. Am. Chem. Soc.* **2018**, *140*, 4774-4777.

[6] A. Colubri, A. K. Jha, M. Y. Shen, A. Sali, R. S. Berry, T. R. Sosnick, K. F. Freed, *J. Mol. Biol.* **2006**, *363*, 835-857.

[7] G. G. Krivov, M. V. Shapovalov, R. L. Dunbrack, *Proteins* **2009**, *77*, 778-795.

[8] S. A. Izmailov, I. S. Podkorytov, N. R. Skrynnikov, *Sci. Rep.* **2017**, *7*, 9293.

[9] T. J. Dolinsky, P. Czodrowski, H. Li, J. E. Nielsen, J. H. Jensen, G. Klebe, N. A. Baker, *Nucleic Acids Res.* **2007**, *35*, W522-W525.

[10] H. Nguyen, D. R. Roe, C. Simmerling, *J. Chem. Theory Comput.* **2013**, *9*, 2020-2034.

[11] R. Friedman, E. Nachliel, M. Gutman, *Biophys. J.* **2005**, *89*, 768-781.

[12] J. P. Ryckaert, G. Ciccotti, H. J. C. Berendsen, *J. Comput. Phys.* **1977**, *23*, 327-341.

[13] S. Piana, K. Lindorff-Larsen, R. M. Dirks, J. K. Salmon, R. O. Dror, D. E. Shaw, *PLoS One* **2012**, *7*, e39918.

[14] P. F. Batcho, D. A. Case, T. Schlick, *J. Chem. Phys.* **2001**, *115*, 4003-4018.

[15] H. J. C. Berendsen, J. P. M. Postma, W. F. van Gunsteren, A. Dinola, J. R. Haak, *J. Chem. Phys.* **1984**, *81*, 3684-3690.

[16] D. Van der Spoel, E. Lindahl, B. Hess, G. Groenhof, A. E. Mark, H. J. C. Berendsen, *J. Comput. Chem.* **2005**, *26*, 1701-1718.

[17] S. You, H. Lee, K. Kim, J. Yoo, *J. Chem. Theory Comput.* **2020**.

[18] D. A. Case, *Accounts Chem. Res.* **2002**, *35*, 325-331.

[19] W. H. Press, S. A. Teukolsky, W. T. Vetterling, B. P. Flannery, *Numerical Recipes in C*, Cambridge University Press, Cambridge, **1992**.

[20] P. Virtanen, R. Gommers, T. E. Oliphant, M. Haberland, T. Reddy, D. Cournapeau, E. Burovski, P. Peterson, W. Weckesser, J. Bright, et al., *Nat. Methods* **2020**, *17*, 261-272.

[21] A. G. Palmer, *Chem. Rev.* **2004**, *104*, 3623-3640.

[22] A. G. Palmer, *Annu. Rev. Biophys. Biomol. Struct.* **2001**, *30*, 129-155.

[23] D. Schneidman-Duhovny, M. Hammel, J. A. Tainer, A. Sali, *Biophys. J.* **2013**, *105*, 962-974.

[24] I. K. McDonald, J. M. Thornton, *J. Mol. Biol.* **1994**, *238*, 777-793.

[25] J. L. Bentley, *Commun. ACM* **1975**, *18*, 509-517.

[26] K. Kämpf, S. A. Izmailov, S. O. Rabdano, A. T. Groves, I. S. Podkorytov, N. R. Skrynnikov, *Biophys. J.* **2018**, *115*, 2348-2367.

[27] T. I. Yusufaly, Y. Li, G. Singh, W. K. Olson, *J. Chem. Phys.* **2014**, *141*.

[28] a) D. J. Barlow, J. M. Thornton, *J. Mol. Biol.* **1983**, *168*, 867-885; b) J. E. Donald, D. W. Kulp, W. F. DeGrado, *Proteins* **2011**, *79*, 898-915.

[29] J. Cavanagh, W. J. Fairbrother, A. G. Palmer, N. J. Skelton, M. Rance, *Protein NMR Spectroscopy. Principles and Practice (2nd Edition)*, Academic Press Inc., San Diego, **2007**.

[30] T. D. Yager, C. T. McMurray, K. E. van Holde, *Biochemistry* **1989**, *28*, 2271-2281.

[31] N. P. Hazan, T. E. Tomov, R. Tsukanov, M. Liber, Y. Berger, R. Masoud, K. Toth, J. Langowski, E. Nir, *Biophys. J.* **2015**, *109*, 1676-1685.

[32] A. K. Shaytan, G. A. Armeev, A. Goncearenco, V. B. Zhurkin, D. Landsman, A. R. Panchenko, *J. Mol. Biol.* **2016**, *428*, 221-237.

[33] L. Bintu, T. Ishibashi, M. Dangkulwanich, Y. Y. Wu, L. Lubkowska, M. Kashlev, C. Bustamante, *Cell* **2012**, *151*, 738-749.

[34] T. T. M. Ngo, Q. C. Zhang, R. B. Zhou, J. G. Yodh, T. Ha, *Cell* **2015**, *160*, 1135-1144.